High-capacity Continuous Descent Operations

A case study of Amsterdam Airport Schiphol

K.A. ter Beek

Technische Universiteit Delft

TU Delft

High-capacity Continuous Descent Operations

A case study of Amsterdam Airport Schiphol

by

K.A. ter Beek

For obtaining the degree of Master of Science in Aerospace Engineering
at the Delft University of Technology,
to be defended publicly on Friday April 8, 2022 at 09:00.

Student number:	4290399	
Thesis committee:	Prof. dr. ir. J.M. Hoekstra,	TU Delft, chair
	Dr. Ir. J. Ellerbroek,	TU Delft, supervisor
	Ir. P.C. Roling,	TU Delft, examiner

TU Delft

Preface

For obtaining the degree Master of Science in Aerospace Engineering at the Delft University of Technology. This thesis report discusses High-capacity Continuous Descent Operations at Amsterdam Schiphol Airport. This thesis has been created under supervision of Prof. Dr. Ir. J.M. Hoekstra and Dr. Ir. J. Ellerbroek from the faculty of Aerospace Engineering at the Delft University of Technology.

The report is structured as follows. First, the paper is presented of the final research conducted. Afterwards is the preliminary report in which the initial procedures and experimental setup for the research are discussed.

K.A. ter Beek
Delft, April 2022

I
PAPER

High Capacity Continuous Descent Operations at Amsterdam Airport Schiphol

Kars Andreas ter Beek

Delft University of Technology

Abstract

The International Air Transport Association (IATA) and the European Commission (EC) have stated their desire for the aviation industry to reach net zero carbon emissions by 2050 and in addition these emissions must be reduced by 45% in 2030. In order to reach these goals, all possible contributions to a reduction in carbon emissions are considered. One of these is the Air Traffic Management (ATM) procedure of Continues Descent Operations (CDO). These operations describe a flight path for the approach where there are minimum level flight segments. This paper investigates the maximum possible impact of this procedure for maximum capacity operations. Four different days have been analysed where the individual components of the procedure are investigated; vertical optimisation, lateral optimisation and the combined case. Using ADS-B data from busy days in august of 2019, these procedures are described and simulated using fast-time ATM simulation software Bluesky using Base of Aircraft Data (BADA) performance data and total-energy model. Compared to current operations, vertical optimisation could possibly safe 20% of fuel, lateral optimisation could theoretically safe 16% fuel and the combined case has the potential to safe up to 27% fuel without negatively impacting capacity.

Collaborators: Prof. dr. ir. J.M. Hoekstra, dr. ir. J. Ellerbroek

1 Introduction

In October 2021, the IATA pledged to reach 'net zero' carbon emissions by 2050 which is aligned with the wishes from the EC. Additionally, in 2030 the net carbon emissions must be reduced by 45% compared to the baseline set in 2019. In order to achieve this task, despite an ever growing demand in aviation, a roadmap has been made by Netherlands Aerospace Centre (NLR) and SEO Amsterdam Economics [6]. In this roadmap, it is projected that absolute emissions are reduced by 92% while the remaining 8% is removed from the atmosphere through negative emissions. There are 4 main fields which are key in the reduction of current carbon emissions. According to the roadmap, improvements in aircraft and engine technology will account for 45% of the reduction, improvements in ATM and aircraft operations will account for 7%, using Sustainable Aviation Fuel (SAF) will account for 40% and the remainder will be due to carbon removal projects. All fields must contribute to the eventual goal. In this research, the aircraft operations aspect is determined in one specific field, a possible application of Continues Descent Approach (CDA) at Amsterdam Airport Schiphol (AMS) in high capacity circumstances.

International Civil Aviation Organization (ICAO) defines a CDA as an "operating technique where aircraft maintain a low engine thrust setting, low drag configuration thereby reducing fuel burn and emissions during descent with minimum level flight segments". A study from EUROCONTROL showed that the benefit of continuous descent and continuous climb operations included fuel savings of up to 350,000 tonnes per year[1]. Where the continuous descent phase has ten times the potential benefit then continuous climb operations. This is due to current operations more closely resembling continuous climb operations. In a response to these potential benefits, EUROCONTROL has created a Continues Climb Operations (CCO)/CDO action plan in order to help implement these procedures, showing the urgency of this subject.

CDAs were originally theorised as a noise abatement technique but are currently more widely considered as a fuel saving technique. While CDAs have been shown to be beneficial in numerous studies dating back to 2000[7], it is still quite difficult to fully implement the procedure at high capacity circumstances[9] [4]. For example, AMS only uses CDAs at night during low traffic hours and at a starting altitude of 7,000ft. London Heathrow Airport (LHR) is able to utilise CDAs "over 90% of the time[1]" with the application of holding stacks to sequence aircraft. This negates the fuel and carbon emissions benefits of the CDA. The main consideration for LHR for applying CDO is noise abatement for residents. In order to get a more detailed insight of the full impact of CDAs on the fuel consumption, this research focuses on the implementation of CDAs at AMS during high capacity situations where runways are at their maximum capacity. Additionally, the CDAs will be analysed from cruise altitude to determine the full benefit of the energy saving procedure.
The impact of CDAs on fuel consumption have been analysed theoretically and also by using flight tests. These experiments largely start the CDA at around 7,000 ft [19], [16] and have potential energy savings of the order of 40-50kg for medium sized aircraft [3] and upwards of 400kg for large sized aircraft [12].

[1] eurocontrol.int/concept/continuous-climb-and-descent-operations

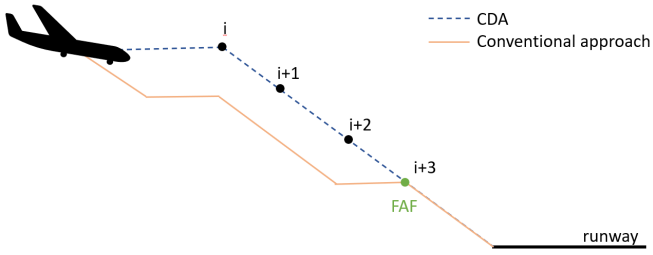

Figure 1: CDA of aircraft

2 Experimental Setup

2.1 Research objective

This research focuses on 'designing a framework for CDO at Amsterdam Airport Schiphol which minimises fuel consumption while maintaining capacity and determining the maximum theoretical impact of the CDO procedure in terms of fuel consumption at AMS'. This consequently means the possibility of redesigning the airspace surrounding AMS in order to fully accommodate the continues descent procedure. Additionally, new airborne and ground systems may be required in order to implement the procedure, so long as the CDO is able to be implemented at high capacity.

2.2 Research setup

In order to analyse the CDO at AMS, the aircraft will be simulated using a real time air traffic management simulator Bluesky[2]. Bluesky is a complete open-source simulation tool created to gain more insight in and to implement new methods for research in ATM. For this research, 5 scenarios are designed.

1. Base case: This scenario serves as the baseline to analyse the impact of the other scenarios
2. CDA scenario: This scenario is the implementation of an optimised vertical path. The lateral path however remains identical to the base case.
3. Lateral scenario: This scenario is the optimised lateral path of the aircraft. The vertical path remains identical to the base case. This means the shortest possible lateral path to the runway.
4. Combined scenario: This scenario is the combined optimised lateral path and the CDA path which is a optimised vertical path.
5. Combined scenario with separation: This scenario is the same as the combined scenario, however with separation implemented for the aircraft.

These scenarios have been designed in order to separate and asses the impact of the individual components of each setup. Therefore, the impact of an optimal vertical path and horizontal path are simulated and analysed separately before they are combined in the last two scenarios.

2.3 Simulation setup

These scenarios will be simulated using Bluesky for four different wind conditions (North, East, South, West) at AMS. The aircraft will be simulated using actual data from aircraft landing at AMS during a busy period in the summer of 2019. The data is gathered from an ADS-B recorder[3] located at the faculty of Aerospace Engineering at the Delft University of Technology. From the busiest data, an arrival peak is chosen for simulation of maximum capacity landing runway usage at AMS. An example of such a peak can be seen in Figure 2 and the corresponding wind vectors for that day in Figure 3.

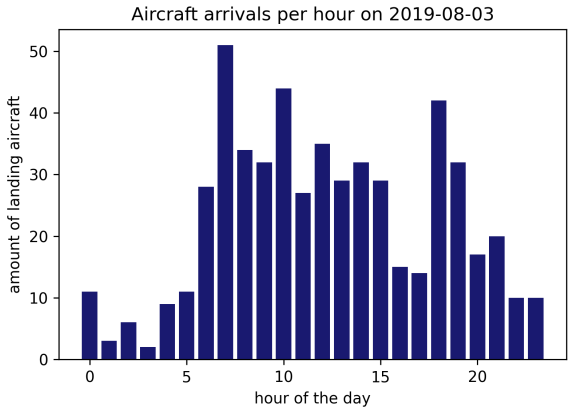

Figure 2: Aircraft arrivals per hour for AMS

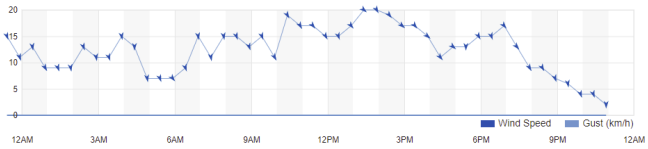

Figure 3: Wind vectors for 2019-08-03[4]

The simulation border is defined by the Top of Descent (ToD) for the aircraft which is determined by the flight path angle and the starting altitude for the descent. The flight path angle is set globally for all aircraft. The FPA has been set at 2.5°similarly to the analysis done by Wu et al [18] based on the ideal fuel minimum FPA and is also based on the research done by Inaad[5] where the fuel optimum FPA has been determined for different aircraft types. This is assuredly not the definitive number for the FPA, but for the consideration of fuel optimum CDAs it is a valid starting point. The starting altitude for the descent has been determined at 10km altitude, around 33,000ft for all aircraft resulting in a ToD for the aircraft at 229km distance from AMS. The simulation dates and wind conditions are listed in Table 1.

Table 1: Dates, wind direction and times used for simulation

Wind direction	Time and date	# aircraft
North	2019-08-03 06:15-7:45	78
East	2019-08-09 6:15-7:45	80
South	2019-08-09 17:45-19:15	75
West	2019-08-05 17:45-19:15	82

[2] https://github.com/TUDelft-CNS-ATM/bluesky
[3] https://surfdrive.surf.nl/files/index.php/s/KYTR1ldO6vqCxXG

2.4 ADS-B data

The ADS-B data is filtered, edited and transformed before being used as the data can have some inaccuracies. The first data point of an aircraft must be at least 100km from AMS, otherwise the extrapolation distance to the ToD border of 229km gets too large causing inaccuracies in the aircraft data. The final data point needs to be within 20km distance from the centre of AMS too make sure that aircraft are landing at AMS. Additionally the data is edited to remove any outlying data points which are obvious recording errors, such as latitude and longitudinal coordinates around the equator which is too far away from the ADS-B receiver to actually phyiscally register. Finally, the aircraft types are added from the hex ICAO code from open sources[5]. When the aircraft type cannot be retrieved a random aircraft is picked from the most prevalent aircraft at AMS[2]. +6

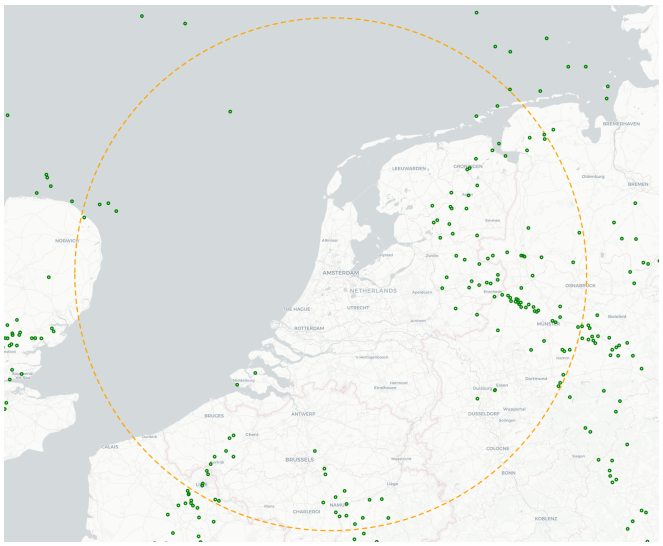

Figure 4: First point of contact with ADS-B receiver

Some aircraft, indicated in green, fall within the ToD circle, indicated in orange, in Figure 4 due to the curvature of the earth and the location of the ADS-B receiver. These aircraft are extrapolated to the border of the ToD for the simulation. Aircraft that are outside the ToD circle are cut-off such that the aircraft is created exactly on the ToD border for all aircraft. Aircraft that are extrapolated to the border are extrapolated based on data from other aircraft within the same route. Occasionally there is data available from aircraft that are flying higher and therefore can send data to the ADS-B receiver from farther away, this gives more insight into the track of aircraft coming from that bearing which is used for extrapolation.

2.5 BADA performance and fuel calculations

Bluesky has two performance models that it can use for its calculations. One is OpenAP[13], an open source aircraft performance database and the other is Eurocontrol's Base of Aircraft Data (BADA v3.12). The BADA model is one of the most used aircraft performance models but it is licensed. Due to the unusual nature of the CDA approach, OpenAP is insufficient in its performance calculations for this type of procedure and as such, BADA is used as the performance model for the simulations. BADA uses a Total-Energy Model which "equates the rate of work done by forces acting on the aircraft to the rate of increase in potential and kinetic energy". Which in the case of an ideal CDA should be as low as possible as the goal is to maximise the potential and kinetic energy that the aircraft has at the ToD.

The equation BADA uses is:

$$(T - D)V_{TAS} = W\frac{dh}{dt} + mV_{TAS}\frac{dV_{TAS}}{dt} \tag{1}$$

Where T = thrust $[N]$, D = drag $[N]$, m = aircraft mass $[kg]$, W = weight of the aircraft$[N]$, V_{tas} = true airspeed $[m/s]$, h = altitude $[m]$, $\frac{d}{dt}$ = time derivative $[s]$. BADA uses fixed coefficients for the drag depending on the flight phase and is a function of the lift coefficient

$$D = C_d * \frac{1}{2}\rho V_{TAS}^2 * S \tag{2}$$

$$C_d = C_{d_0} + k * C_l^2 \tag{3}$$

Where the values for C_{d_0} and k change depending on the flight phase.

$$C_L = \frac{m * g_0}{\frac{1}{2}\rho V_{TAS}^2 * S * cos\theta} \tag{4}$$

With θ the bank angle of the aircraft. Finally, fuel consumption is calculated as follows:

$$\eta = C_{f1}\left(1 + \frac{V_{TAS}}{C_{f2}}\right) \tag{5}$$

Where η = thrust-specific fuel consumption, C_{f1} = TSFC coefficient 1 and C_{f2} = TSFC coefficient 2. Accordingly, the fuel flow is determined using the actual thrust of the aircraft using:

$$f_{nom} = \eta * Thr \tag{6}$$

For the minimum fuel flow, the idle thrust descent conditions are used and is determined using the geopotential pressure H_p altitude by:

$$f_{min} = C_{f3} * (1 - \frac{H_p}{C_{f4}}) \tag{7}$$

This idle thrust part of the descent is generally stopped when the aircraft switches to approach configuration (8,000ft) and landing configuration (3,000ft). The nominal fuel flow after these configurations are enabled is determined using the nominal fuel flow expression given by Equation 6 with a minimum fuel flow of Equation 7.

3 CDA scenario design

The main reason that CDA procedures are difficult to implement is the inability for Air Traffic Control (ATC) to properly space aircraft that are decelerating at different rates, as well as gliding with different velocities due to differing aerodynamics and aircraft weights [9] [4]. At AMS,

[5] www.planespotters.net/

this is currently negated by only implementing CDA procedures at night when there are less flights and hence there is increased spacing between aircraft. Early studies have shown that an ad-hoc implementation of CDA procedures at AMS starting at an altitude of 7,000ft could reduce airport capacity by as much as 50% due to an increase of the landing interval from 1.8min to 4min [7].

3.1 Governing Equations, solid body/-mass

The situation of a descending or ascending flight is given by Figure 5. The governing equations of $F = ma$ for a solid body is described for the horizontal and the vertical plane by Equation 8 and Equation 9.

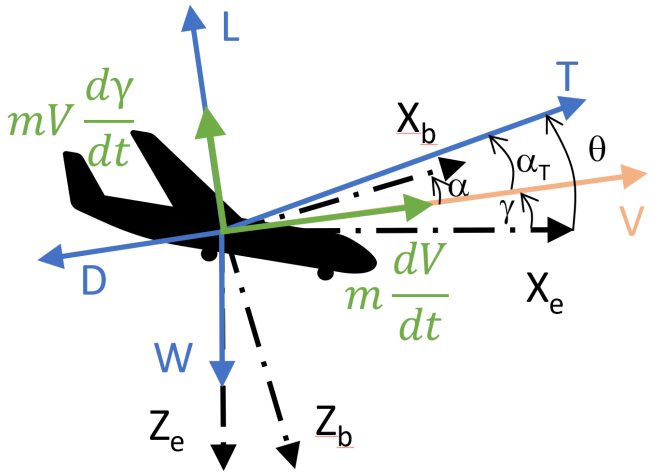

Figure 5: Free body diagram and kinetic diagram of aircraft

Where equilibrium in the horizontal plane is described by:

$$T \cdot \cos\alpha_T - D - W \cdot \sin\gamma = m\frac{dV}{dt} \tag{8}$$

And equilibrium in the vertical plane is described by:

$$L - W \cdot \cos\gamma + T \cdot \sin\alpha_T = mV\frac{d\gamma}{dt} \tag{9}$$

Where α_T = angle of thrust vector [-] is assumed small. In Bluesky, the Thrust is determined from the resultant of the forces of the aircraft. In the case of a CDA, this is should technically be the other way as the Thrust should be set to zero and the resulting of forces results in the flight path of the aircraft. As this is currently not possible, the flight path is predicted preemptively in order for the corresponding resulting Thrust to be zero. This means that the flight path angle and deceleration are the only components to compensate for the Drag, described as following:

$$D = W \cdot \sin\gamma_d + m \cdot a_d \tag{10}$$

Where $\gamma_d = -\gamma$ is the negative flight path angle and $a_d = -a$ is the deceleration.

3.2 Determining CDA profile

In Equation 10, it can be seen that there are three main parameters that determine the horizontal flight path, the amount of Thrust, the flight path angle (either positive or negative) and change of velocity (either increasing, decreasing or steady). As for the CDA the Thrust setting is equal to idle, the remaining components within the equation must be satisfied by either a steeper descent γ_d, or an increase of the deceleration of the aircraft a_d. This shows the described issues with the CDA, the flight trajectory for the aircraft (speed profile based on a_d and altitude profile based on γ_d) is mainly dependent on the aircraft mass and aerodynamic drag. Thus, for each aircraft, the flight trajectory can be determined based on these parameters. In Figure 6, the impact of these parameters is analysed for a fixed altitude for an Airbus A320. From this, the nominal impact of the amount of Thrust can be observed and the significant impact of the deceleration of the aircraft it has on the glide slope.

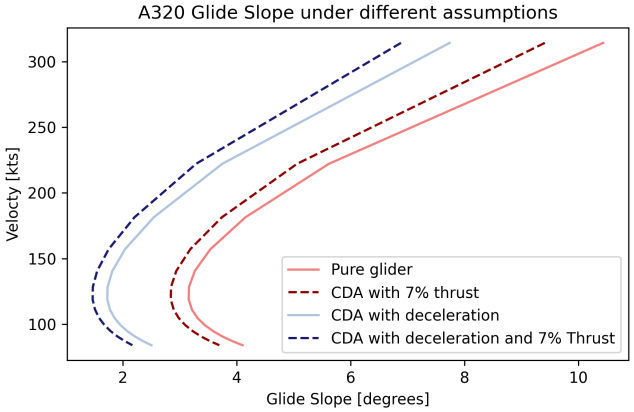

Figure 6: Aircraft FPA difference

For this research, the flight path angle is determined globally for all aircraft based on research which showed that for a decelerating flight from cruise, a flight path angle of 2.5°is beneficial for most aircraft [5] [15] [18]. In previous studies it is stated that a constant FPA provides positive results as well [4] [14]. Based on the FPA, the ground distance required for descent from cruise to the Final Approach Fix (FAF) can be determined by:

$$d_{descent} = \frac{alt_{cruise} - alt_{approach}}{tan\gamma} \tag{11}$$

3.3 Velocity profile

When the ground distance for descent is required, the velocity profile can be determined. This in term determines the moment to start descent along the aircraft track. For the deceleration a_d it is assumed that the aircraft has a constant deceleration from the starting point of the descent to the FAF. The deceleration can then be determined by:

$$a = \frac{V_{cruise}^2 - V_{approach}^2}{2 * d_{descent}} \tag{12}$$

As mentioned, the flight trajectory must be determined preemptively and then given as commands to aircraft in Bluesky as described in Figure 1.

The descent starts at point i based on $d_{descent}$, the required deceleration across the descent is given by $-a = a_d$ and the vertical speed must be determined for each section between i and $i + n$. The velocity at point $i + n$

is determined by:

$$V_{i+1} = \sqrt{V_i^2 + 2 * d * a} \tag{13}$$

Therefore, the vertical speed can be determined by averaging the speed along each segment and multiplying it with the sine of the flight path angle. Because the vertical speed is averaged along each segment and the velocity is slowly decreasing along each segment, the actual FPA of the aircraft is an approximation of the predetermined FPA by being too shallow in the beginning of each segment and too steep at the end of each segment. However, this variation is relatively small and the FPA hovers between 2.45°and 2.55°as a result. The difference between the flight path and fuel consumption of the CDA scenario and the base case is shown in Figure 7 and Figure 8. From Figure 8, it is noticeable that during descent the fuel flow is at idle levels and increases only with the geopotential pressure as described in Equation 7. Compared to the base case where each slight deviation from the vertical slope is causing an increase in fuel flow. Conversely, the extended cruise segment is also clearly noticeable in the fuel flow and causes and increase of fuel consumption for the CDA scenario in the beginning.

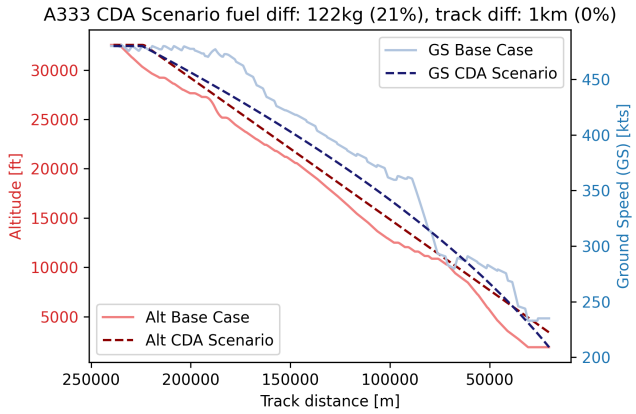

Figure 7: CDA Scenario comparison with Altitude and Ground Speed

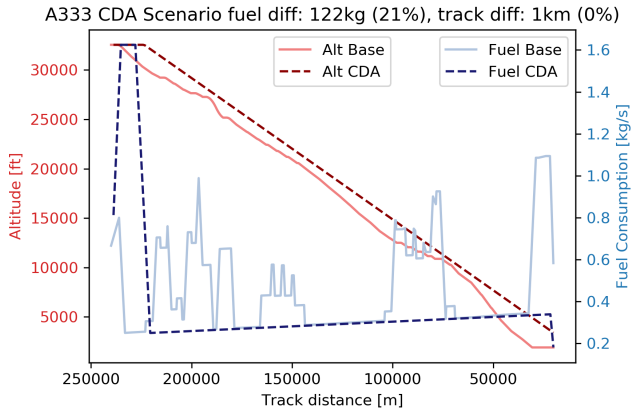

Figure 8: CDA Scenario comparison with Altitude and Fuel Consumption

4 Lateral scenario design

In order to analyse the impact of a combined free flight scenario and CDA, the individual impact of the lateral shortest path must be determined. First, the FAF are established for each runway. From the FAF, every aircraft will have the same final approach path to the runway. This is due to safety concerns which are mainly focused on aircraft having non-idle thrust at the final approach for possible a possible go-around and also to compensate for mandatory flap settings that are required for landings. Hence the analysis of the performance of the CDA are all until the FAF is reached. After that the flight path will continue with the current standard procedures. The FAF is established at a 3°glide slope in order to intercept the ILS at an altitude of 3,500ft meaning it is 20.4km from the start of the runway (radius R). This also means that for the scenario with separation implemented, all aircraft must be sufficiently separated at the FAF.

4.1 Route to FAF

The routes of aircraft to the FAF can be separated into two variants, aircraft that can fly directly to the FAF and aircraft that need to traverse along the FAF circle to the FAF point. This difference is indicated in Figure 9. If an aircraft has an angle to the FAF point of larger then 90°, then the aircraft needs to traverse the FAF circle in order to reach the FAF.

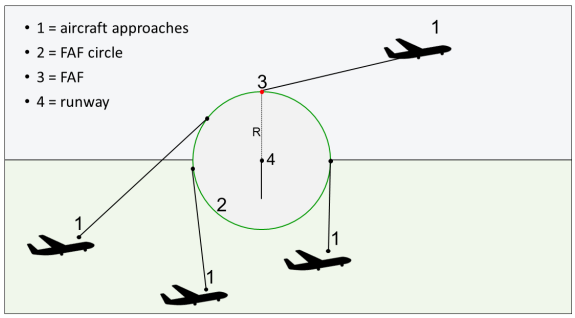

Figure 9: Example of route to FAF

Aircraft fly either directly to the FAF or the FAF circle. Every 1000m a waypoint is generated along this route with the corresponding latitude and longitude. Along the FAF circle, aircraft traverse the circle with radius R and an angle change of 1°per waypoint and these are then plotted along the route on the FAF circle until the FAF is reached. Correspondingly, aircraft need their respective altitude and velocity for each waypoint. The altitude and velocity of aircraft are determined relative to the track distance to AMS compared to the Base Case. By doing so, horizontal flight sections are still part of the flight trajectory as well as deceleration segments. This is done intentionally to be able to analyse the impact of decrease in flight distance on its own without altering the altitude and speed profile too much.

When applied to the total traffic for a scenario, the difference in tracks can be observed in Figure 10. Due to the implementation of the new FAF, some aircraft have an increased track distance for the flight to AMS. This is due to the location of the FAF for the Base Case, for RWY06 and RWY36R it is at 2,000ft, 11.5km away from the runway. Thus aircraft in the Base Case that had no path stretching from ATC are travelling a shorter path then the approach proposed here.

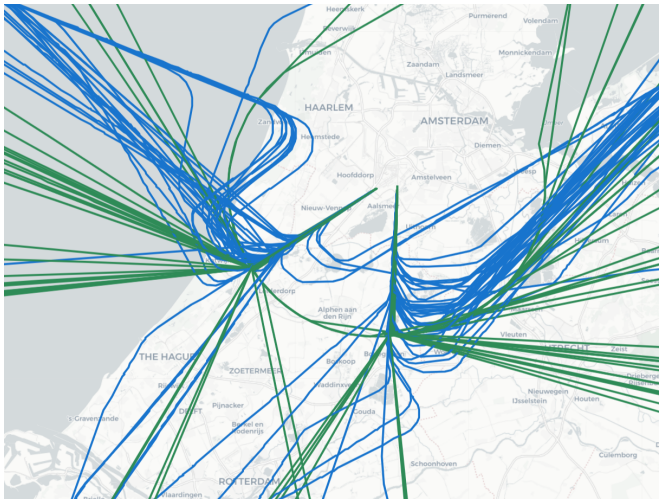

Figure 10: Example of Lateral Case (green) compared to Base Case (blue)

5 Combined scenario and separation

The combined scenario implements both the optimum vertical path of the CDA and the optimum horizontal path with the shortest path to the FAF. For separation, Time-Based Separation (TBS) is used where aircraft are separated based on their respective ETA to the FAF. The separation time between aircraft is determined to be 120 seconds per aircraft. This is a simplification of current practices using TBS where there are combinations of wake-vortex categories which dictate the separation time. LHR takes this even a step further by implementing Enhanced Time-Based Separation (eTBS) with even closer separation requirements increasing landing rates during light wind conditions to 40-46 landings per hour where pair wise separation is implemented creating a matrix of 96x96 possible aircraft pair possibilities [1]. When compared to regular conditions at AMS, 120 seconds on average is a close approximation of the current maximum sustained landing rate of 68 landings per hour for two runways [8] and therefore a conservative estimate of the potential capacity of the airport when applying TBS. It must be noted that for TBS and potentially eTBS, the aircraft mix of the airport is a major influence on the capacity which is unfavourable for AMS due to its relatively large amount of small aircraft landing at the airport.

In Table 2, an example is given of this process. The delay time must be added to each aircraft in order to maintain separation at the FAF. Because the flight path is pre-determined per aircraft, and the aircraft can not be delayed after the descent has started at the ToD, the aircraft must be delayed by extending its flight path during the cruise phase. This extension is thus a delay of the start of the descent. The distance to be added to the track of the aircraft is then equal to the delay time divided by the cruise speed.

Table 2: Aircraft ETA example

Aircraft ETA	Delta [s]	Delay [s]	Net Delay [s]
AC1 14:05:20	-	-	-
AC2 14:06:00	40	(120-40)	80
AC3 14:06:30	30	(120-30)+80	170
AC4 14:08:30	120	(120-120)+170	170
AC5 14:13:50	320	(120-320)+170	-

The new extended path is determined based on the two scenarios described in subsection 4.1. The distance is added by either increasing the radius of the FAF circle as shown in Figure 11, or by extending the FAF in the runway direction as shown in Figure 12. For increasing the radius, the distance added as determined by the net delay time is described by the following:

$$D_2 = \Omega * R_2 + (R_2 - R_1) + (\frac{k}{cosf} - k) \tag{14}$$

With small angle assumption for f and assuming constant velocity for the extended path and t_1 is the regular travel time for distance D_1 and t_2 is the required delay time as determined by the ETA, the path can be described as:

$$V(t_1 + t_2) = \Omega * R_2 + (R_2 - R_1) \tag{15}$$

Solving for a new required radius for the FAF circle leads to:

$$R_2 = R_1 + \frac{V * t_2}{1 + \Omega} \tag{16}$$

Where R_2 is the new FAF circle radius and Ω the radial travelled along the FAF circle. The new route is then plotted for each degree change along the radial for the new radius as described in subsection 4.1.

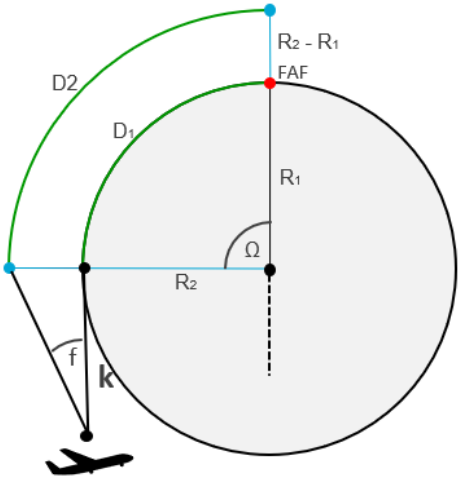

Figure 11: Extended path along FAF Circle

For the other situation, aircraft are extended by placing the FAF further backward. This path extension is determined by choosing an appropriate angle α which extends the path by $D + k_2 - K - 1$. Along k_2 and D waypoints are created every 1000m. Along these waypoints the altitude, vertical speed, and velocity is created as described in subsection 3.2.

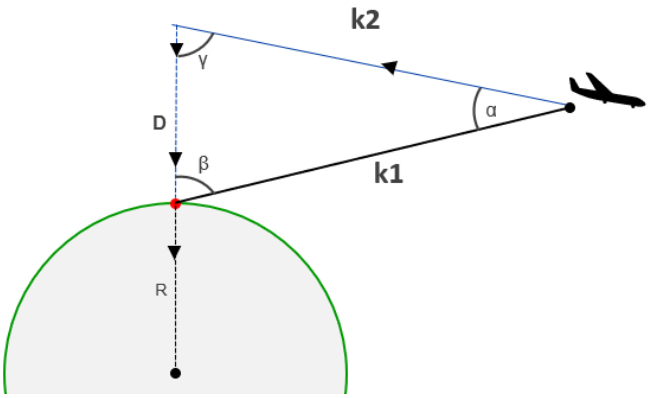

Figure 12: Extended path by increasing FAF distance

In Figure 14, the overview of the new paths is shown. In comparison with the overview of the aircraft routes for the base case visualised in Figure 13, it is clear that the tracks of the aircraft cover a larger area then the conventional tracks. The path extension for separation can also clearly be observed with clear corridors of aircraft for the path extension described in Figure 12.


Figure 13: Aircraft routes for the Base Case. Altitude is indicated by the color scheme.


Figure 14: Aircraft routes for the Combined Case. Altitude is indicated by the color scheme.

6 Results

From the described design of the scenarios, the results can be observed in Table 3, Table 4 and Table 5. Do note that the handles are shortened: SCN1 through SCN5 are respectively the base case scenario, the CDA scenario, the Lateral scenario, the Combined scenario and the Combined scenario with separation. The scenarios have been simulated with four different wind conditions, North, East, South and West. The scenarios are analysed on three parameters, total fuel consumption in order to investigate the potential fuel savings and environmental impact, total distance travelled to determine the relative effectiveness of shortening the lateral path and total distance travelled below 7,000ft in order to analyse the impact in terms of noise where it is considered a hindrance when aircraft are flying below 7,000ft [1] [17].

Table 3: Total fuel consumption per scenario

Fuel [kg]	SCN1	SCN2	SCN3	SCN4	SCN5
North	52,967	44,795	47,839	45,203	56,190
East	56,696	45,711	45,894	39,591	47,075
South	69,207	50,478	56,150	44,345	56,288
West	56,890	47,631	46,698	42,149	51,738

Table 4: Total distance travelled per scenario

Distance [km]	SCN1	SCN2	SCN3	SCN4	SCN5
North	19,640	19,405	18,176	18,773	20,786
East	21,102	21,004	18,514	19,411	20,852
South	21,838	21,755	19,038	20,040	21,868
West	22,553	22,477	19,995	21,006	22,719

Table 5: Total distance travelled below 7,000ft per scenario

Dist.< 7,000ft [km]	SCN1	SCN2	SCN3	SCN4	SCN5
North	4,361	3,504	3,886	3,567	3,630
East	5,236	3,554	4,487	3,687	3,530
South	5,584	3,790	4,904	3,827	3,643
West	5,694	3,829	4,941	3,889	3,705

6.1 CDA Scenario

The CDA scenario compares the impact of an optimised vertical path to the base case scenario. For this scenario, the fuel consumption is on average decreased by 20% for the analysed segment. For the total of 315 flights analysed for the different conditions this corresponds to an average fuel savings of 150kg of fuel and 474kg of CO_2 per flight for the simulated section. This corresponds with the current findings from literature [5] [10] [4] [16]. It is noted however that the fuel savings is not distributed evenly among aircraft types, some aircraft, such as the B747-400, save a significant larger amount during the descent phase then other aircraft as the B733. The difference between aircraft is further explained in detail in Table 6.

In terms of total distance travelled, this scenario performs almost identically to the base case due to travelling the same lateral path. However, the distance travelled below 7,000ft is decreased due to the more efficient vertical path. The horizontal segments of the flight path have been eliminated which leads to a 30% decrease of flight segments below 7,000ft. This could have a potential significant impact on noise for residents of the area near the airport, however it is difficult to state the exact impact of this due to the difficulty of determining specific noise sources of an aircraft and the corresponding experience of the noise on the residents. Separation has not been taken into account for this scenario as this would impact

the analysis off the vertical path. As the only manner of ensuring separation for this scenario would be adjusting the flight speed during the descent which counters the concept of an ideal CDA.

6.2 Lateral Scenario

The lateral scenario compares the impact of the shortest lateral path to the base case scenario. For this scenario, the fuel consumption is on average, decreased by 16%, for the total number of flights this is corresponds to fuel savings of 120kg of fuel and 379kg of CO_2 per flight. The lateral path is 11% shorter compared to the Base Case, saving around 30km per aircraft. The main reason for a larger decrease in fuel is the shortened cruise phase, as the path is shortened the aircraft has to cruise for a smaller distance before starting the descent. This means that in general, a larger amount of fuel is saved then purely related to the distance that is saved.

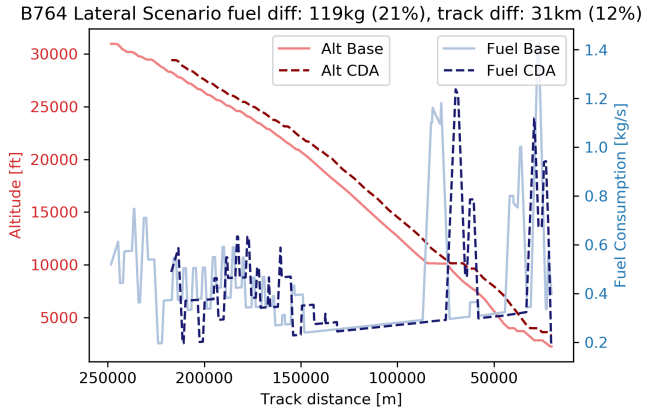

Figure 15: Fuel consumption Lateral Scenario

This process can clearly be seen in Figure 15, where the segment at high altitude uses considerable fuel burn. After this segment, fuel idles at some stages before a horizontal segment is started. Fuel burn follows the same pattern for the Lateral Scenario as the Base Case but the main difference lies in the starting segment of the aircraft. Separation for this scenario has also not been taken into account to be able to independently analyse the impact of the shortest lateral path. Ensuring separation with this scenario compared to the base case would mean adjusting the velocity profile. This would impact the fuel consumption for this scenario due to factors other then the decrease in flight distance and would therefore impact the comparison to the base case scenario.

6.3 Combined Scenario

The Combined Scenario is split into two different scenarios, one with and one without separation applied. The scenario without separation applied could be considered as the ideal case for the future. As aircraft scheduling and ATM concepts become more accurate for example with the full deployment of SESAR[6]. This means that aircraft could be accurately sequenced and spaced before they even arrive in the airspace and once they arrive in the TMA, the path to the FAF is the optimised lateral and vertical path for the aircraft. No further path stretching or delays would be required in order to sequence and space aircraft. Potential conflicts that may arise in aircraft with vastly differing glide slopes and glide velocities can easily be negated by small deviations in the lateral path from ToD to the FAF. Although this is currently not yet possible, it is considered the theoretical maximum possible benefit of an optimised vertical and lateral path. This theoretical maximum benefit in terms of fuel consumption is around 27%, or around 200kg of fuel and around 632kg of CO_2 per flight for the segment within the TMA.

For the combined case with separation, aircraft are spaced and sequenced based on the arrival schedule from the Base Case scenario. The fuel savings for this scenario are on average 10% which comes down to around 75kg of fuel and 237kg of CO_2 per aircraft. The total distance travelled is almost 2% larger then the Base Case. However, the total distance travelled below 7,000ft is 30% smaller than the Base Case. Additionally, it can be noted that the distance saved by creating a shortest lateral path is negated by the distance added in order to delay the aircraft for appropriate separation. Secondly, due to this increase in distance during the cruise phase in one instance the fuel consumption is larger then that of the Base Case, namely for the North wind condition. As explained in subsection 6.6, this can be explained by the relatively straight path that aircraft traverses to the final approach fix. The distance saved by the shortened lateral path is minimal. The impact of this can be seen in the distance added due to separation, around 2000km. The main consideration is that the distance added in order to delay the aircraft, is travelled at cruise speed. Whereas cruise speed if often optimised for maximising the amount of fuel burned per distance travelled $\frac{kg}{m}$. However, as the goal of the path extension is to delay the aircraft, the fuel per second must be minimised in order to delay the aircraft with as little impact on fuel consumption as possible. As this is not the case in this scenario, the path extension has a considerable impact on the total fuel consumption.

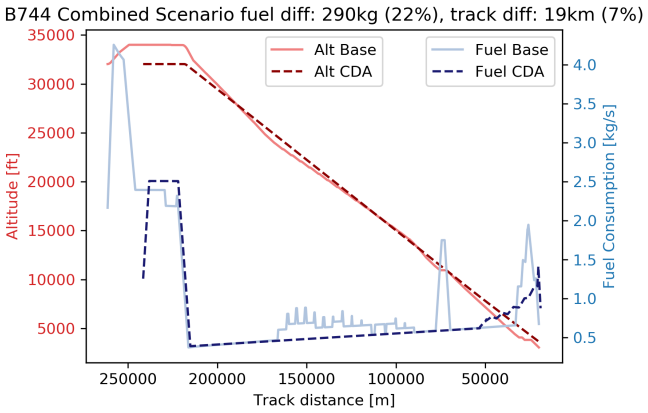

Figure 16: Fuel Consumption Combined Scenario without separation

This is best explained using one aircraft as an example of this process. In Figure 16, the fuel consumption is plotted for a B744 which shows a 22% fuel savings

[6] https://www.sesarju.eu/projects/start

and a 7% savings in distance. When looking at the same aircraft for the case of separation in Figure 17, the distance covered compared to the Base Case is increased by 5km, thus around 24km of distance is added to the cruise phase of the flight in order to delay the aircraft. This has considerable impact on the fuel consumption of the aircraft and almost all benefits gained from implementing the CDA and the optimised lateral path are negated by this increase in cruise flight.

In terms of separation, the scenario ensures separation due to the differing lateral paths of the aircraft. Each aircraft has an almost unique lateral path, as well as a unique vertical path. As such, potential conflicts due to significant differences in aircraft glide path and glide velocity as described in [9] and [7] are negated while the capacity can be maintained from the base case scenario. While the current implementation of separation is an ad-hoc implementation on current flights, the potential fuel savings are even more significant when aircraft are better spaced and separated before they enter the airspace. The maximum benefit of this is described by the combined CDA and lateral scenario without separation.

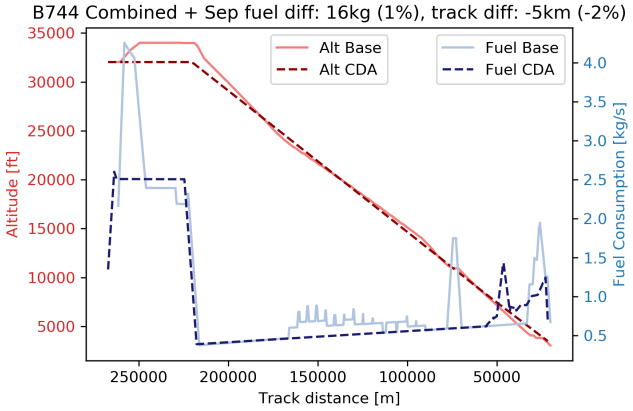

Figure 17: Fuel Consumption Combined Scenario with separation

6.4 Fuel consumption per aircraft

Too gain more insight into the effect of the fuel savings, the fuel savings per aircraft type are listed in Table 6 for the Base Case, CDA Scenario and the combined scenario. This makes for easier comparison with literature where CDAs have been analysed. When comparing the fuel savings per aircraft type with previous studies using fuel optimum CDAs from cruise altitude[5], the fuel savings are similar but appear to be relative conservative to the theoretical fuel savings determined in the study. Most aircraft save between 50 and 100kg of fuel for the CDA scenario, except the larger aircraft which can save over 400 kg of fuel during this phase. To give perspective to these numbers, a Boeing 737-800 aircraft takes around 4600kg of fuel to travel to the south of Spain. The potential fuel savings that could ideally be reached with the proposed combined scenario therefore consists of around 2% of its total fuel consumption. When such an aircraft has to taxi to runway 18R, it has to take around 200kg of taxi fuel with it, a considerable amount as well in regards to its total fuel consumption, there it once again stipulates the importance of reducing fuel consumption on all aspect of aircraft.

Table 6: Average fuel consumption in [kg] per aircraft type

AC type	#AC	SCN1	SCN2	SCN4
B738	94	490	427	378
B744	58	1,663	1,253	1,153
B737	31	414	353	316
A320	28	438	362	314
A319	18	467	405	355
B739	14	478	367	330
A333	12	690	526	540
E190	10	353	320	278
A332	7	846	785	728
B772	6	805	668	628

6.5 Travel time per aircraft

In Table 7 the travel time can be observed. While this has no immediate impact on the performance of the scenarios, it is interesting to note the significant time benefit that the Lateral scenario generates but is fully compensated when this scenario is combined with the CDA implementation. This indicates that the main benefit to the time is the speed profile of the aircraft that matches the Base Case.

Table 7: Average time travelled within the TMA

	SCN1	SCN2	SCN3	SCN4	SCN4 SEP
time [s]	1,673	1,593	1,446	1,611	1,696

6.6 Differences between the simulation days

From Figure 18 and Figure 19, the difference in days can be observed. Whereas aircraft from Figure 19 are flying relatively straight to the FAF, the aircraft in Figure 18 are vectored a considerable amount and the path stretching is considerable, this is especially clear at SUGOL. The segments of horizontal flight, indicated in grey, is a logical consequence of the increased vectoring of the aircraft and has a large impact on the scenarios as well. The easier aircraft are able to fly straight to the FAF, the lesser the impact of lateral optimisation is. That the aircraft from the day shown in Figure 19 are flying relatively straight forward can be seen by the distance travelled per aircraft for each scenario for the Base Case in Table 8.

Table 8: Overview of distance travelled per aircraft, Base Case

Wind direction	# aircraft	Dist. [km]	$\frac{Dist.}{ac}$ [km]
North	78	19,640	252
East	80	21,838	273
South	75	21,102	281
West	82	22,553	275

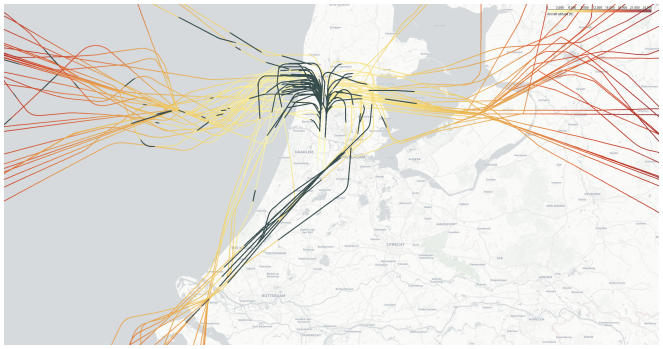

Figure 18: Base Case routes overview, East

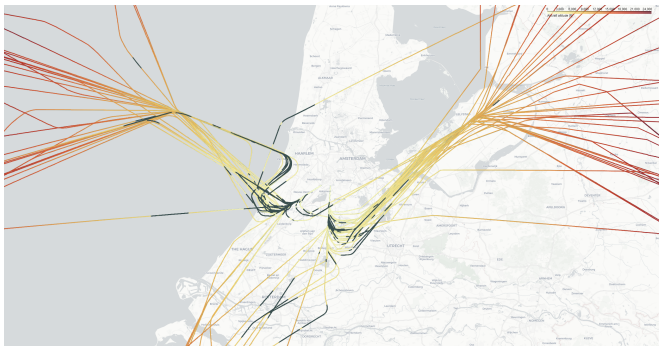

Figure 19: Base Case routes overview, North

7 Discussion

7.1 CDA Scenario

In the generated CDAs of the aircraft, the ideal CDA is not incorporated in this paper. Ideally, this would be implemented by determining the ideal FPA for each segment based on the aircraft mass, drag at each altitude and the deceleration. While it is not implemented in this scenario, the proposed solution allows for this implementation. It must be noted however that a varying glide slope per aircraft may introduce other difficulties. Because smaller aircraft are generally descending less steep then larger aircraft, they might travel below the trajectory of a previous larger aircraft. Considering wake-vortex categories used for TBS, this may induce additional problems due to the nature of wake-vortices travelling downwards. This could in turn mean additional time between these aircraft is required, or alternatively, the smaller aircraft could maintain current separation standards but the must follow the flight trajectory of the leading aircraft.

Also, while wind is taken into consideration in the runway layout of AMS, it is not taken into account during the descent of the aircraft. As the data recorded by the ADS-B receiver is ground speed, this can also be compensated for. However, for full implementation of CDAs in the future, it is required for ATC to have full wind data across the different altitudes for the aircraft to account for this during the calculations of the trajectory.

7.2 Lateral Scenario

As shown in Figure 10, some aircraft have an increased flight path compared to the Base Case due to the distance of the FAF compared to the runway. It could be argued to decrease the distance of the FAF in order to more closely match current operations. However, the FAF radius of the Lateral Scenario has been determined in accordance with the separation design for the combined case. When the FAF radius becomes too small, aircraft will be flying too close too each other and make the final merging to the FAF too cramped in order for ATC too maintain a appropriate separation.

7.3 Combined Scenario

As described in subsection 6.3, there are instances where the added distance required for separation have a significant impact on fuel consumption, even to the point where it increase the total fuel consumption to be larger than the Base Case. This is an unfortunate side-effect of sticking with a fixed vertical trajectory for the aircraft, when lateral flight is no option after the descent has started. Either the velocity profile must be changed during the descent, meaning the trajectory is no longer an ideal CDA descent or the CDA must be aborted and segments of horizontal flight must be adapted. Lastly, the delay could be implemented differently as well by not simply adding a distance at cruise velocity but by forcing the aircraft to decelerate during this phase as well and therefore increasing the delay time over a shorter distance travelled, ideally creating a segment of flight which minimises fuel flow over time.

Additionally, the corridors created for the situation of path extension as described in Figure 12 could in some cases create the scenario that aircraft with different velocity profiles during the descent are running into each other. The proposed lateral shortest path causes lateral separation as well as vertical separation of the aircraft. However, the corridors do not have lateral separation and therefore may creating instances of aircraft running into each other. It would therefore be more desirable to design the corridors per aircraft type as defined by the wake-vortex categories. As such, these aircraft have a similar descent profile due to being in a similar weight class and this effect can be negated again.

7.4 Fuel consumption

As discussed, the fuel consumption uses the BADA model for fuel consumption. As the module for BADA uses quite some assumptions for the flight phases of aircraft, it could be argued that these calculations are not always accurate. Especially when taking into account the flight manoeuvres which are at the moment unconventional. Due to assuming certain flap settings when the aircraft flies below certain altitude, therefore increasing the drag, the calculations stated in this research might be a conservative estimate. It must be noted though that the main impact on the fuel consumption for this research is the descent from cruise altitude to the FAF at 3,500ft, thus the impact of certain flight phases at 8,000ft is considered limited but nonetheless not none.

Additionally, it can be noted that the impact of CDAs during the descent is a nominal amount with respect to the total fuel consumption of an aircraft. However, as aviation has the goal to be sustainable in 2050m it has to take any means necessary in order for it to reach this

goal.

7.5 ATC and pilot execution

During the analysis of the current proposed flight trajectory, departing flights are not taken into account. Also arriving flights at neighbouring airports are not taken into account. Due to the additional area that the aircraft are covering in the proposed solution, this is an import aspect to take into account. While the goal was to look for an ideal solution for landing aircraft at AMS, this may be hindered by other airports.

In the instance a go-around is required, the benefits of the CDA are negated. While this is a safety concern that is taken into account by having a final approach similar to current procedures, re-entering the airspace to land a second time is not as straight forward as it is more difficult to define standard procedures as aircraft are more freely using the airspace. The same holds for the implementation of holdings stacks.

Similarly, pilots must be able to execute the proposed procedure for CDO. While not straightforward, there have been some studies which investigate the pilot workload during the CDA where the main focus point lay on the communication between the projected aircraft track and how the pilots can navigate this. Including vertical speed commands. This has been studied in [11] where 'descriptive waypoints' were implemented in order to provide the pilots targets and feedback along the CDA path which resulted in a successful following of the CDA path for the pilots.

8 Recommendations

This research has shown a proof of concept for the application of CDAs during high capacity situations at AMS. For future studies it would be recommended to implement the ideal fuel optimised CDA for each individual aircraft based on the aircraft mass, drag and deceleration instead of implementing a global solution. In addition, it is recommended to implement RECAT-EU wake-vortex categories for TBS. It is also recommended to implement more corridors to the FAF such that aircraft with significant different trajectories and speed profiles can overtake and stay at their ideal glide path.

For future studies into CDAs it would be recommended to get a more accurate basis for the aircraft data as the ADS-B data can have quite some discrepancies which need to be accounted for. Also it would be interesting to gain the insight of an approach controller on the current status of the design. While several meetings were held with commercial pilots in order to get an insight on the feasibility of the designed approach procedures, the insight of an approach controller would be beneficial as well.

Additionally, it would be interesting to further analyse the potential trade-offs for delaying the aircraft in the cruise phase of flight or between decelerating additionally during the descent as proposed by [9], where fuel consumption is the key driver in the determination of the proposed solution.

Finally, for AMS in the future the following is recommended in order to implement these procedures. The aircraft mix at AMS currently features quite some smaller aircraft when compared to other large airports such as LHR which has quite some success with implementing CDAs, albeit from a limited altitude. Due to having a large mix of aircraft types, separation using TBS will be more difficult to implement due to more restriction in the differing wake-vortex categories. When more aircraft of a similar type are landing, the separation constraint will be more favourable and thus the capacity can be increased. This could be of considerable impact when large scale CDAs are implemented. As AMS is already limited by the number of movements per year, it would be a logical step to shift the balance of these movements more towards heavier aircraft.

In order to implement the proposed solutions for CDAs, ATC needs to have more information available then is possible at the moment. In order to fully calculate the trajectory of the aircraft, ATC must known the aircraft weight, wind vectors across the projected trajectory and ATC must be able to communicate the proposed trajectory clearly with the pilots. Not only must the FMS be able to follow the commands to the way-points as if they are programmed way-points, the pilots must know the route as well in order to verify the flight path during descent as an added layer of safety.

In order to do so, all aircraft within the TMA must give feedback on wind speeds to ATC automatically such that an accurate wind grid can be created with variations between the different flight levels. Technically, it would already be possible to provide pilots with the corresponding way-points for their trajectory using Controller-pilot data link communications (CPDLC). However, this would increase the workload of ATC significantly and thus this should be automated.

9 Conclusion

This research analysed the theoretical possibility of the impact of full CDA operations starting from cruise altitude at AMS during maximum capacity usage of the runways. In order to analyse the problem, ADS-B data was used from actual flights during peaks in the summer of 2019. For these peaks, the aircraft have been optimised on 2 levels, vertical optimisation by implementing the CDA, lateral optimisation by navigating directly to the FAF and the combined case. When aircraft are separated laterally, the implementation of CDAs becomes much more feasible during high capacity circumstances then previously determined as aircraft with significant different speed profiles during their descent trajectory are able to pass without causing a conflict. This in terms means that implementing CDAs would not necessarily negatively impact capacity of airports if this system is used. However, when the ideal trajectory of the CDA is not to be impacted, separation of aircraft at the FAF must be maintained by path stretching before that ToD. This path stretching at cruise altitude has significant impact on the fuel consumption and may in some instances negate the positive impact of CDAs on the fuel consumption.

However, this paper concludes that when aircraft are separated and sequenced before they enter the TMA, the

ideal case fuel savings would be in the order of 27% for the descent flight, averaging at around 200kg of fuel and 632kg of CO_2 per flight. In the case of less ideal separation before the TMA, the aircraft must extend its path in order to be properly separated at the FAF. This implementation would entail fuel savings of 10% on average, around 75kg and 237kg of CO_2 per flight.

AMS	Amsterdam Airport Schiphol
ATC	Air Traffic Control
ATM	Air Traffic Management
BADA	Base of Aircraft Data
CCO	Continues Climb Operations
CDA	Continues Descent Approach
CDO	Continues Descent Operations
CPDLC	Controller-pilot data link communications
EC	European Commission
eTBS	Enhanced Time-Based Separation
FAF	Final Approach Fix
IATA	International Air Transport Association
ICAO	International Civil Aviation Organization
LHR	London Heathrow Airport
NLR	Netherlands Aerospace Centre
SAF	Sustainable Aviation Fuel
TBS	Time-Based Separation
ToD	Top of Descent

References

[1] Noise. URL https://www.heathrow.com/company/local-community/noise/operations/arrival-flight-paths.

[2] B. Bouwels, J.M. Hoekstra, and J. Ellerbroek. Off-idle continuous descent operations at schiphol airport, Apr 2021. URL http://resolver.tudelft.nl/uuid:fa55d141-ea6d-4bb9-b463-515742e55935.

[3] Yi Cao, Daniel DeLaurentis, and Dengfeng Sun. Benefit and trade-off analysis of continuous descent approach in normal traffic conditions. *Transportation research record*, 2325(1):22–33, 2013.

[4] John-Paul B Clarke, Nhut T Ho, Liling Ren, John A Brown, Kevin R Elmer, Kwok-On Tong, and Joseph K Wat. Continuous descent approach: Design and flight test for louisville international airport. *Journal of Aircraft*, 41(5):1054–1066, 2004.

[5] J. Ellerbroek, Mazin Inaad, and J.M. Hoekstra. Fuel and emission benefits for continuous descent approaches at schiphol, Nov 2016. URL http://resolver.tudelft.nl/uuid:85153290-ac20-4005-8901-60d3861a8c75.

[6] NLR Nederlands Lucht en Ruimtevaart Centrum. A route to net zero european aviation, Feb 2021. URL https://www.destination2050.eu/wp-content/uploads/2021/02/Destination2050_ExecutiveSummary.pdf.

[7] Louis Erkelens. Research into new noise abatement procedures for the 21st century. 2000. doi: 10.2514/6.2000-4474.

[8] Mike Fairbanks, Ference van Ham, and Ference Choroba. Second opinion on the application of cdas at schiphol airport final report, 9 2008. URL www.askhelios.com. Producedfor the Ministry of Transport, Netherlands.

[9] W. F. De Gaay Fortman, M. M. Van Paassen, M. Mulder, A. C. In't Veld, and J. P. Clarke. Implementing time-based spacing for decelerating approaches. *Journal of Aircraft*, 44:106–118, 2007. ISSN 15333868. doi: 10.2514/1.22253.

[10] S. Khardi. Aircraft shortest and fastest continuous descent approach development. *Journal of Aircraft*, 49, 2012. ISSN 15333868. doi: 10.2514/1.C031775.

[11] Michael LaMarr, Nhut Ho, Walter Johnson, and Vernol Battiste. Enhancing pilot ability to perform cda with descriptive waypoints, Oct 2011. URL https://ieeexplore.ieee.org/abstract/document/6096102.

[12] Kevin R Sprong, Kathryn A Klein, Camille Shiotsuki, James Arrighi, and Sandy Liu. Analysis of aire continuous descent arrival operations at atlanta and miami. In *2008 IEEE/AIAA 27th Digital Avionics Systems Conference*, pages 3–A. IEEE, 2008.

[13] Junzi Sun, Jacco M. Hoekstra, and Joost Ellerbroek. Openap: An open-source aircraft performance model for air transportation studies and simulations. *Aerospace*, 7(8), 2020. ISSN 2226-4310. doi: 10.3390/aerospace7080104. URL https://www.mdpi.com/2226-4310/7/8/104.

[14] Kwok-On Tong, Ewald G Schoemig, Danial A Boyle, Julien Scharl, and Aslaug Haraldsdottir. Descent profile options for continuous descent arrival procedures within 3d path concept. In *2007 IEEE/AIAA 26th digital avionics systems conference*, pages 3–A. IEEE, 2007.

[15] Daichi Toratani, Navinda Kithmal Wickramasinghe, Jendrick Westphal, and Thomas Feuerle. Feasibility study on applying continuous descent operations in congested airspace with speed control functionality: Fixed flight-path angle descent. *Aerospace Science and Technology*, 107:106236, 2020. ISSN 1270-9638. doi: https://doi.org/10.1016/j.ast.2020.106236. URL https://www.sciencedirect.com/science/article/pii/S1270963820309184.

[16] Enis T Turgut, Oznur Usanmaz, Ali Ozan Canarslanlar, and Ozlem Sahin. Energy and emission assessments of continuous descent approach. *Aircraft Engineering and Aerospace Technology*, 2010.

[17] Anthony Warren and Kwok On Tong. Development of continuous descent approach concepts for noise abatement. volume 1, 2002. doi: 10.1109/dasc.2002.1067906.

[18] Minghong G Wu, Steven M Green, and James Jones. Strategies for choosing descent flight-path ... - arc.aiaa.org, Oct 2014. URL https://arc.aiaa.org/doi/full/10.2514/1.C032835.

[19] Busink J.J. Wubben, F.J.M. Environmental benefits of continuous descent approaches at schiphol airport compared with conventional approach procedures. 2000.

II
PRELIM

Contents

List of Tables

List of Figures

ADS-B Automatic Dependent Surveillance-Broadcast

AMS Amsterdam Airport Schiphol

ATC Air Traffic Control

ATM Air Traffic Management

ATS Air Traffic Services

CCO Continues Climb Operations

CDA Continues Descent Approach

CDO Continues Descent Operations

DBS Distance Based Separation

eTBS	Enhanced Time-Based Separation
FAF	Final Approach Fix
FMS	Flight Management System
FPA	Flight Path Angle
GBAS	Ground Based Augmentation System
GFS	Global Forecast System
ILS	Instrument Landing System
KPI	Key Performance Indicator
LAX	Los Angeles International Airport
LHR	London Heathrow Airport
LVNL	Luchtverkeersleiding Nederland
MLW	Maximum Landing Weight
MTOW	Maximum Take-Off Weight
OEW	Operational Empty Weight
STAR	Standard Terminal Arrival route
TBS	Time-Based Separation
TDDA	Three-degree Decelerating Approach
TMA	Terminal Control Area
ToD	Top of Descent

1
Introduction

Even amidst a global pandemic such as the one as the time of writing, the global aviation industry remains fairly optimistic about future growth, albeit somewhat delayed. Eurocontrol projects that the 2019 level of air traffic will return in 2024 or later [5] and in the long run, growth is expected to return to pre-COVID levels [6]. Simultaneously, the Dutch government is working on a plan on redesigning the Dutch airspace for the ever changing demand of the airspace. The key components of this are to increase efficient use of the limited Dutch airspace and to help make aviation more sustainable [7]. So, even though it is a less pressing issue at the time, it remains ever important in the future to further reduce fuel and noise emissions from aircraft.

In order to decrease the impact of aviation on the environment, several measures can be taken. Designing more sustainable aircraft, using bio-fuels or electric propulsion but also from an operational perspective improvements can be made. Most likely, a combination of all of the above will be the best solution in order to reduce the most emissions. In this research, the operational perspective will be investigated in order to decrease emissions from the aviation industry in the future. The main focus of this research will be on the Terminal Control Area (TMA) and the descent and approach manoeuvres of aircraft. More specifically, the Continues Descent Operations (CDO) and the Continues Climb Operations (CCO). CDO is used interchangeably with CDA and this procedure is defined by International Civil Aviation Organisation [18] as the following:

> "CDO is an aircraft operating technique aided by appropriate airspace and procedure design and appropriate Air Traffic Control (ATC) clearances enabling the execution of a flight profile optimised to the operating capability of the aircraft, with low engine thrust settings and, where possible, low drag configuration, thereby reducing fuel burn and emissions during descent. The optimum vertical profile takes the form of a continuously descending path, with a minimum of level flight segments only as needed to decelerate and configure the aircraft or to establish on a landing guidance system (e.g. Instrument Landing System (ILS))".

CDO is frequently mentioned in literature and Air Traffic Services (ATS) as a promising method to reduce both emissions and noise nuisance during the landing phase of the aircraft [7] [17]. This maneuver is said to be beneficial for residents living in close proximity to the airport due to a reduction in pollution and noise, but also for airliners as it can potentially save on average 174 kg of fuel per flight compared to current operations [11]. However,this approach procedure is not yet the industry standard and is not widely implemented for high capacity operations at the moment due to the complexities concerning this maneuver because of separation concerns and corresponding capacity at the airport. Currently at Amsterdam Airport Schiphol (AMS), CDO are used during the night when there are few aircraft. According to early studies, the uncertainties during the approach phase require an increase in separation time from 1.8 minutes to 4 minutes; a decrease in capacity of over 50% [13]. While airliners have an intrinsic motivation to safe fuel and thus money, they are often limited in performing the CDA in the TMA due to restrictions imposed by ATC.

CCO are more widely used and are mainly limited by speed restrictions and levelling off sections due to airspace restrictions. When these restrictions are lifted, aircraft could more steadily climb towards their cruise phase, saving on average around 40kg of fuel per flight at AMS [12].

While the research on CDO / CCO operations is promising in terms of fuel savings, procedure wise it encounters more difficulties. This research will focus on the complexities of implementing these two manoeuvres at AMS and will aim to design procedures facilitating these manoeuvres in order to maximise fuel savings while

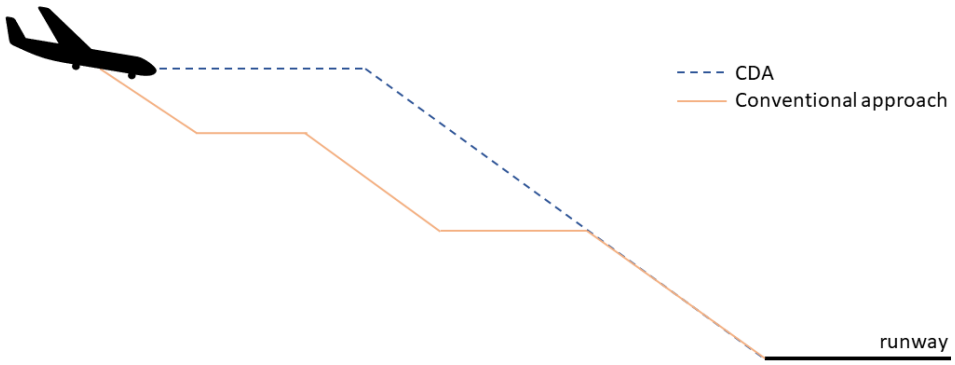

Figure 1.1: Basic principle of a CDA

maintaining key Key Performance Indicator (KPI)'s for AMS such as capacity and safety. Simultaneously recommendations will be made for future systems, both airborne and on the ground which may facilitate the proposed procedures. As the outcome of this research may be relevant to designing future procedures at AMS, transparency is of the utmost importance. As such only open source software, data and tools are used to ensure that every reader is able to reproduce the results presented in this research.

2
Background and Literature Review

In this chapter, more information is provided on the intricacies of operations at AMS. Similarly, relevant research is presented which may aid in a possible solution. In section 2.1, more background information is given on current operations at AMS. In section 2.2 more information is given on recent literature on CDO.

2.1. Background AMS

This research focuses on a practical implementation of CDO and CCO at AMS. As such, it is important to identify what makes AMS different from other airfields around the world. AMS is one of the few airports that does not make use of Standard Terminal Arrival route (STAR). In order to get a better grasp on the complexities of designing routes for AMS, an interview was setup with someone at Luchtverkeersleiding Nederland (LVNL) who is involved in the current process of redesigning the Dutch airspace. The interviewee highlighted some core operation parts and related issues which highly influenced the design process of AMS. Among these issues are (in no specific order): the varying wind direction and velocity, the runway layout, AMS its hub function and corresponding inbound and outbound peaks, noise restrictions for residents nearby meaning 14 to 17 runway changes per day, the amount of flights per day and the opening of Lelystad airport. Accounting for all of these factors during the redesign of AMS for CDO and CCO are considered out of scope, but the factors that are considered within scope will be described in the following sections.

2.1.1. Wind directions and runway layout

AMS has a unique and to some extend dated runway layout. The most common used runway layout at AMS is the parallel layout, as this makes dealing with traffic easier as less aircraft routes are crossing when changing the active runways. However, the disadvantage is that aircraft are more heavily influenced by cross-winds. Therefore, airport runways are always built in the most predominant wind direction for that area. AMS has three parallel runways (18L, 18C and 18R (and the other way around)) and three additional runways covering most other directions. As such, during heavy winds, there is always an airstrip available which lets aircraft land relatively close to a full on headwind leading to a decreased amount of crosswind and a more safe and easy approach.

However, there are quite a few limitations in the runway usage of AMS. The most prominent limitations will be described, with the main focus on noise nuisance from residents. To decrease the amount of noise that residents are exposed to per day or per week, AMS must vary the usage of runways accordingly, to distribute noise more evenly. Therefore, it is not always possible to use the runway that has the best orientation with respect to the wind. Due to this requirement, AMS must switch runways resulting in increased complexity in terms of aircraft arrivals.

When observing and comparing the wind roses from some large airports around the world with AMS, a few interesting things can be noted. When comparing AMS to Los Angeles International Airport (LAX) as seen in Figure 2.1 and Figure 2.2, AMS has substantial more varying wind directions and more intense wind velocities. Compared to LAX, the runways have a less logical orientation with respect to the wind. Also, the wind intensity at LAX is significantly lower. When comparing this further with Figure 2.4 and Figure 2.3, the same uniformity in wind directions can not be noted for London Heathrow Airport (LHR) as aircraft land more often with crosswinds.

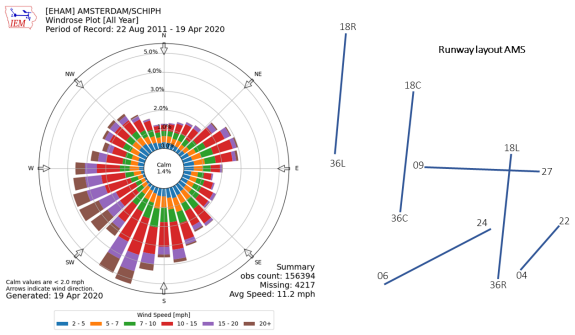

Figure 2.1: Runway layout and Wind rose of AMS ©Iowa Environmental Mesonet

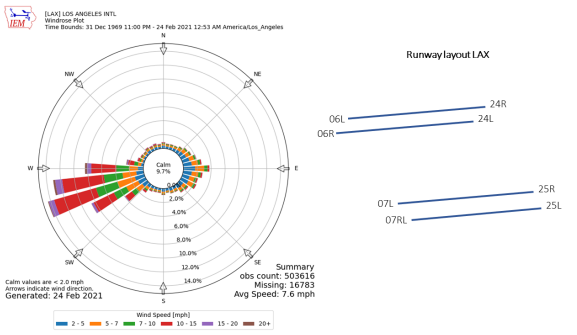

Figure 2.2: Runway layout and Wind rose of LAX ©Iowa Environmental Mesonet

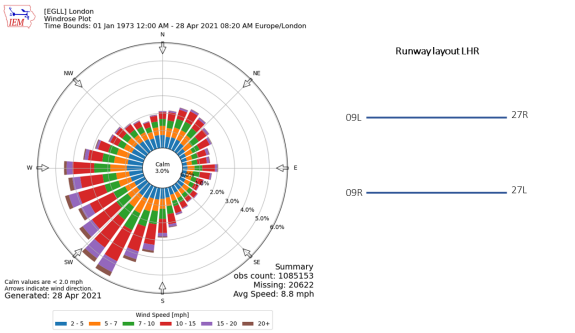

Figure 2.3: Runway layout and Wind rose of LHR ©Iowa Environmental Mesonet

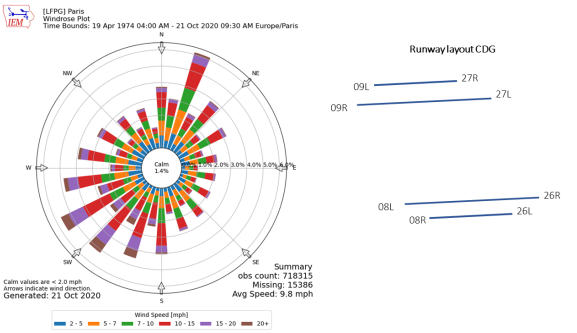

Figure 2.4: Runway layout and Wind rose of CDG ©Iowa Environmental Mesonet

2.1.2. Inbound and outbound peaks and approaches

Another difficulty at AMS is the main function as a HUB airport resulting in large inbound and outbound peaks. These consist of two morning peaks (one inbound and outbound), two afternoon peaks and one evening peak. During a large inbound peak, for example between 7 am and 9 am, there are often more than 60 landing aircraft and during an outbound peak, for example between 9 am and 11 am, there are the same amount of departing aircraft. This means that the runway configuration must change quickly during this switch between inbound and outbound.

Currently, AMS uses no fixed approaches. ATC vectors the aircraft from their final point from the STAR and guides to aircraft to the Final Approach Fix (FAF). In Figure 2.5, this is visualised from the different directions. However, it should be noted that for the airspace redesign, a 4th approach fix is considered from the south-east that passes Utrecht. Before FAF, the aircraft often has a section of level flight as this is easier for ATC, and makes interception of the ILS more easy as the ILS is intercepted from below. In the charts of the instrument approaches, this level segment is given in Figure 2.6.

2.2. Literature Review

This section will explain the intricacies of the use of CDO, possible solutions and the current research gap.

2.2.1. Benefits of CDO and CCO

CDA is a procedure which has been described for some time. In the past it was mainly described as a noise abatement technique [13], but over the last 10 years or so, it is also increasingly mentioned as a fuel saving technique [11]. Most recently, Eurocontrol widely supports this procedure in order to get more airports in Europe to adapt this approach technique [15].

The benefits of implementations of CDO throughout Europe are well-defined by Eurocontrol and are identified as :

1. A decrease of 340,000 tonnes of fuel
2. A reduction of over 1 million tonnes of CO_2 emissions

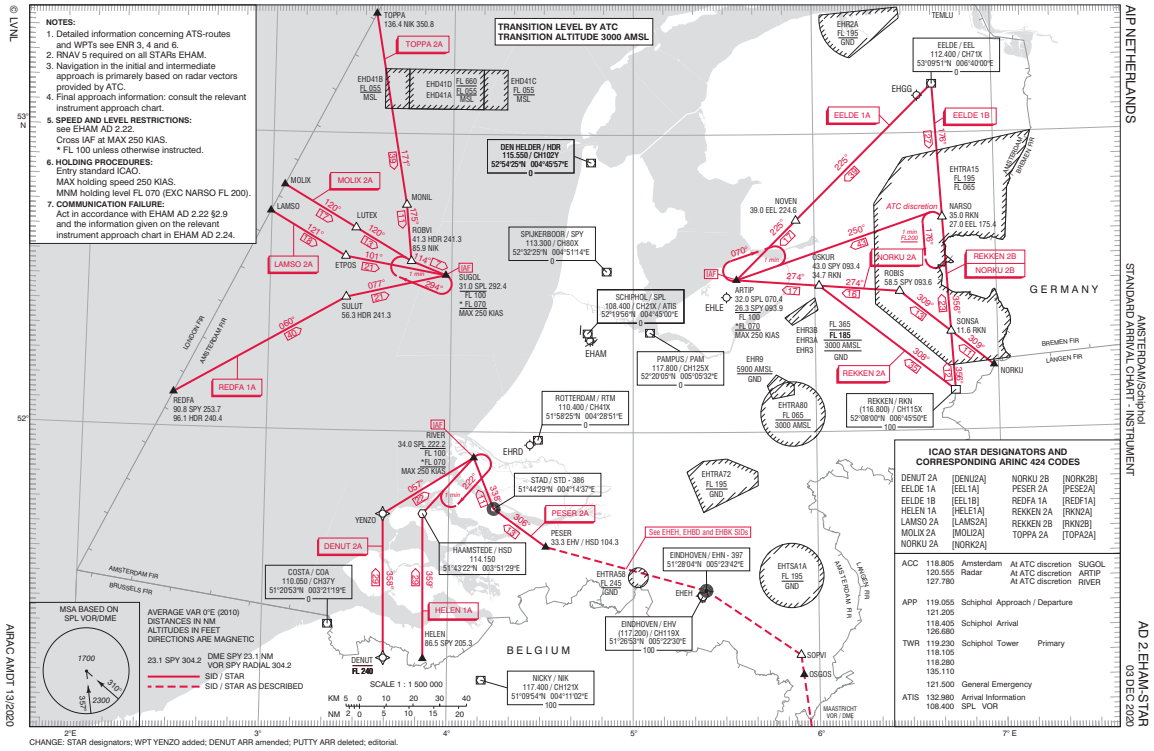

Figure 2.5: Current STAR at AMS ©LVNL

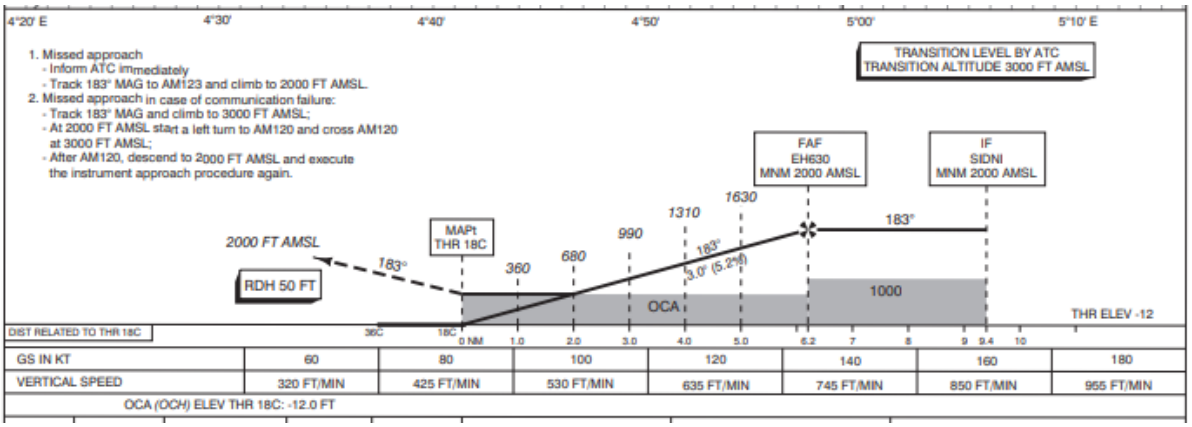

Figure 2.6: Instrument Approach chart VOR runway 18C ©LVNL

3. A reduction of 1 to 5 dB noise pollution around the airport due to decrease in level flight segments
4. A saving of around 150 million euros on fuel

Currently however, according to Eurocontrol, only 41% of flights in Europe are a CDO from FL75 (the top of the noise CDO) and only 24% fly a CDO from Top of Descent (ToD) (the top of fuel CDO). Deployment of optimised CCO and CDO throughout Europe will be beneficial to all European ATM system stakeholders and will help the network to address the environmental challenges it faces.
To further encourage and help airports implement CDA as a standard, Eurocontrol has published a European CDO / CCO Action Plan [15] to "call for and commit to, a step change in the facilitation, promotion and implementation of CCO/ CDO with the objective of significantly reducing noise and CO_2 emissions".

2.2.2. Difficulties of CDO and CCO

This method of approach for aircraft is however not yet the industry standard, due to a number of complexities concerning this maneuver. The problem of spacing during the descent phase consists of three parts: varying wind conditions, aircraft with different deceleration/glide profiles, and inconsistent pilot behaviour. They all contribute to the uncertainty in the approach trajectory and in the long run, this makes it particularly challenging for air traffic controllers to place aircraft in space [17].

Studies at AMS have shown that an ad hoc implementation of CDA reduced airport capacity by as much as 50% [13]. Due to the increased uncertainty during the approach, more spacing is required between aircraft which decreases the capacity significantly. As wind is of major influence on the optimum FPA, AMS is relatively more influenced by this which makes implementation more difficult [17]. A Three-degree Decelerating Approach (TDDA) is proposed, which is mainly focused on noise abatement by creating a flap scheduling algorithm to decrease noise. However, the procedure requires an altered screen for the pilot in order to know when to deploy flaps or additional thrust. Additionally, the pilot workload was considered too high in cases of more severe wind conditions.

LHR is one of the airfields that is able to fully implement CDO and is able to successfully facilitate CDO in 87% of the time [3]. In order to do this, LHR uses some advanced systems in place which help ATC implement CDA at almost all times. LHR uses Time-Based Separation (TBS) or Enhanced Time-Based Separation (eTBS) instead of Distance Based Separation (DBS), that is currently used at most airports. This is due to the fact that it is harder for the controller to 'see' the separation if it is based on time than a fixed distance on the screen [30]. Because of this, a special screen has been developed for ATC to help assist with the maneuver. LHR also uses Recat-EU, a re-categorisation of wake vortex classes for aircraft and separation requirements between categories. LHR uses pairwise separation identifying more then 96 aircraft categories to further aid in maintaining an as safe as possible and close distance between aircraft further increasing capacity [4]. Furthermore, LHR makes extensive use of holding stacks in order to properly sequence aircraft and starts the CDA at 6,000ft or 7,000ft altitude. It should be noted that the benefits of the CDA in terms of fuel may be offset by the increased fuel usage in the holding stacks. In terms of noise, this type of operations is still beneficial. Lastly, it should be noted that LHR is one of the busiest two runways airports in the world. Due to this, the slots for landing are quite expensive and the types of aircraft landing at LHR are generally more of the same larger categories then other airports.

2.2.3. Different types of CDO

There are also different types of CDO that can be performed, the simplest of which would be a standard fixed three degree FPA approach. This approach is an extension of the ILS, where the Flight Management System (FMS) can follow both the designed vertical and horizontal path. However, this is not a 100% optimal CDO as each aircraft has a different aerodynamic flight path and wind is a major factor in this. If aircraft have a less steep aerodynamic FPA they cannot fly with idling engines and are therefore consuming more fuel than would be considered optimal. The added benefit would be the possibility of decelerating the aircraft by decreasing thrust resulting in more control for ATC.

An alternative to this is the Aerodynamic Flight Path Angle approach. This approach causes a FPA for the aircraft for which the descent is optimum in terms of fuel consumption and the relative aerodynamic FPA to the aircraft. This optimum FPA is unique for each aircraft due to various aerodynamic differences between aircraft types, flight configuration, wind speed, but also across one single aircraft type due to the differing weights of the aircraft during landing. All of these factors combined determine the actual FPA of the aircraft. Part of the difficulty with this is that not all these factors are known to ATC and therefore currently unable to accurately be determined by ATC. A benefit to this aerodynamic FPA is that it results in a more predictive ground speed and therefore eliminating part of the extra required separation that is currently in place for constant FPA CDA [19].

While most of the above mentioned factors influencing the aerodynamic FPA can be known or estimated, the aircraft weight is very difficult to determine as this is not yet communicated between tower and pilot. An aircraft can be almost empty during the landing phase and close to Operational Empty Weight (OEW) or can have almost full tanks and close to Maximum Take-Off Weight (MTOW). This creates difficulty for the air traffic controller as any speed or altitude commands during the glide phase would contradict the benefits of a optimum CDO.

2.2.4. Proposed solutions

Separation in the sky has been proposed by Veldt, 2004 [30], with the addition of an extra screen and a wind prediction algorithm [17]. This would aid the pilot in maintaining the three degree glide slope while the pilot is also able to decelerate using control surfaces and thus maintaining separation with other aircraft. This would require all aircraft to be retro-fitted with such a display, pilot training and of course the requirement to have this display when an aircraft wants to land at AMS. Pilot workload appeared to be a large concern for the authors due to the addition of an additional display. However, workload for the controller was not found to be a limiting factor [17].

From a more technical and airspace design approach, Alam 2011 [8] proposed a discretisation of the TMA into concentric cylinders with artificial way-points and proposes to use an elimination algorithm based on the aircraft performance envelope from one way-point to another to identify all possible routes. From these resulting possible routes, the final route is selected based on a trade-off on noise, emission and fuel consumption. This has been simulated in an air traffic simulator for Sydney Australia TMA. The proposed routes show a 15% reduction in noise, 11.6% reduction in NO_x emission and 1.5% reduction in fuel. The relatively smaller fuel consumption can be explained by the fact that aircraft are flying a longer distance, as it flies in circles above the runway, instead of a more direct path to the runway.

In Sáez, 2020 [28] the authors proposed a mixed-integer programming approach to compute aircraft arrival routes in a TMA creating Merge Trees with proper separation and time to the runway arrival. In this merge tree, all aircraft are assumed to be flying their optimal CDA and do not use any speedbrakes. This study is very interesting and poses an interesting solution to the problem. In terms of a more optimum solution, this approach leads to less distance being flown and has a focus on robustness. The previously mentioned problems however of not knowing weights is not yet solved though and also computing time using this solution is an issue and makes actual implementation not yet possible.

Part of possible solutions to a more efficient airspace at AMS as currently recommend in [7] is the fourth approach fix that would aid the TMA of AMS and proposes fixed arrival routes instead of radar vectoring. This would allow for a more structured approach of the TMA, less workload for ATC and more efficient approaches, but also decreasing flexibility for controllers. The complete opposite of this concept would be a complete free flight. To be able to implement this, complete airborne separation of aircraft would be done from the cockpit with new systems in place. ATC would only be there for monitoring. This has been elaborately described by [27].

Point Merge systems could also be a key in maintaining separation between aircraft, while also being able to implement CDA at AMS. This could be implemented in the arrival management as recommended by [10], who proposes a point merge system based arrival management for AMS for one single and one dual runway configuration. A fuel reduction is seen, due to the implementation of CDA, between 14% and 33% compared to the current situation while simultaneously also increasing capacity marginally with around 2 to 9%. Another proposed point merge technique from [14] is a methodology for automated generation of efficient curved CDA trajectories supported by arrival flow merging techniques, resulting in considerable fuel consumption benefits of up to 30%. In addition to this, Ground Based Augmentation System (GBAS) could also be used as an added accurate and more technologically advanced landing system at airports [16]. GBAS is, even compared with ILS, more beneficial to implement at small airports [2] and worth the financial investment compared to ILS, while also having more benefits in terms of technological advancements.

Ideally, this research proposes a combination of techniques and systems that would be required for AMS to be able to use almost 100% CDO at 100% capacity. Additionally, this research would indicate the maximum achievable benefits of CDO implementation at AMS in terms of fuel consumption at the peak level of flight in 2019.

3
Research Plan and Methodology

A primary part of this research is to execute and report the research in such a way that it can easily be reproduced by people reading this research. Therefore, it is imperative to make use of open source data and tools. This originated during redesigning the Dutch airspace called Programma Luchtruimherziening [7] and the desire to gain insight on the theoretical maximum benefits and disadvantages of CDO compared to current operations. To gain more insight into the impact that this has on both fuel consumption and capacity, this research was founded. The main research question and sub-questions are explained in section 3.1, the scenarios that are designed to answer the questions are explained in section 3.2 and finally more in-depth knowledge about the intricacies of CDO is given in section 3.3.

3.1. Research Question, Aim/Objectives and Sub-goals

In this section the main research question is posed as well as the sub-questions which are required to answer the main research question. Additionally the research objective is formulated.

3.1.1. Research Question

The main research question of this thesis is:

> "What is the maximum achievable efficiency in terms of fuel savings and maximum achievable capacity by implementing CDA approaches at Amsterdam Schiphol Airport from the beginning of the TMA using the latest Air Traffic Management (ATM) concepts and airborne systems".

In order to answer the research question, several sub-questions need to be answered:

1. What is the current level of fuel consumption at AMS during peak arrival hours and the corresponding capacity?
2. What is the impact on implementing fuel optimum CDO while maintaining the current lateral path at AMS during peak arrival hours and the corresponding capacity?
3. What is the impact of an optimal horizontal path on the fuel consumption while maintaining the current vertical path at AMS during peak arrival hours and the corresponding capacity?
4. What is the impact of a 4^{th} approach fix, as proposed by the Programma Luchtruimherziening [7], on the fuel consumption and capacity at AMS?
5. What airport requirements must be met in order to implement maximum efficient Continues Descent Operations at AMS?
6. What are the airborne requirements that must be met in order to implement maximum efficient Continues Descent Operations at AMS?

These questions will be evaluated on the parameters: fuel consumption, capacity, robustness and separation. Robustness will be determined based on a differing arrival schedule then previously assumed and the corresponding variations in arrival times in the TMA and the impact it has on the capacity and fuel consumption.

3.1.2. Research Objective

The main research objective of this thesis is:

> "To design a framework for CDO / CCO at Amsterdam Schiphol Airport which minimises fuel consumption while maintaining capacity in the TMA by means of open source tools in order to be able to fully reproduce the results presented in this thesis to aid policy makers in their decision making".

To achieve this goal, a baseline must be set for current fuel consumption levels during an inbound peak of traffic at AMS. From this baseline, extensions must be made in terms of implementing CDA procedures in order to determine the maximum possible efficiency if all flight utilised CDO, this will serve as the maximum achievable fuel savings, and subsequently likely reduced capacity at AMS. After this, separation and proper procedures must be closely investigated in order to stay as close a possible to this maximum achievable fuel savings while simultaneously increasing capacity. Safety, remains a primary condition at all times.

Finally, a trade-off will be made in terms of maximum efficiency of fuel savings and capacity. The research 'gap' is that so far, there is no real analysis on hypothetical potential fuel benefits at AMS and the corresponding capacity. In literature is often stated that CDO will be a benefit in terms of emissions and noise, but this can range from 1% to 20% and is often not specific on the corresponding capacity. This research may aid policy makers to set more clear targets in terms of fuel reductions at AMS and the corresponding capacity as well as give more insight to the trade-off between these that is inherent to the problem. This research also seeks to help create clearer targets for the operational side of the aviation industry to achieve zero emissions by 2050.

3.2. Scenario setup

The research question and sub-questions posed can be answered using real-time simulation in Bluesky[1]. Bluesky is a complete open-source simulation tool created to gain more insight in and to implement new methods for research in ATM developed by Prof. Dr. Ir. J.M. Hoekstra and Dr. Ir. J. Ellerbroek from the Delft University of Technology. In this thesis, 5 scenarios are designed in order to answer the above mentioned research questions. These scenarios consist of the following:

- Scenario 0: This is the baseline scenario and is simply a simulation of real life air-traffic based on ADS-B data of a busy day in the summer of 2019. This will serve as the baseline scenario and is a scenario where the airport is functioning at almost 100% capacity.
- Scenario 1: This scenario is a vertical optimisation of the baseline scenario. It is vertically optimised by implementing CDO and keeping the same lateral path as the baseline scenario. This scenario will be split into two separate sub scenarios: First, an optimum sub scenario where separation will be ignored to purely look at the potential benefit of an optimal CDA. Second, a sub scenario where separation will be maintained between aircraft to look at the practical implementation of CDO for the scenario. The second sub scenario will also give relevant information on capacity.
- Scenario 2: This scenario is a horizontal optimisation of the base case scenario and keeps the same vertical path as the base case scenario.
- Scenario 3: This scenario implements a 4_{th} approach fix as proposed in the Programma Luchtruimherziening [7]. The vertical path will remain the same as the base case scenario.
- Scenario 4: The ideal case. This scenario will be an optimisation of both the horizontal and vertical path while maintaining proper separation in order to give an estimate of the performance of CDO and CCO at AMS.

A large influence on the eventual capacity is the actual implementation of maintaining separation. This mainly relies on the implementation of point merge techniques and the possibility of implementation of airborne separation systems and more accurate time-based prediction methods for ideal CDO / CCO at AMS. During testing of the scenarios it will be determined whether these techniques and systems will be beneficial, and to what capacity, for the eventual fuel consumption and capacity.

[1] https://github.com/TUDelft-CNS-ATM/bluesky

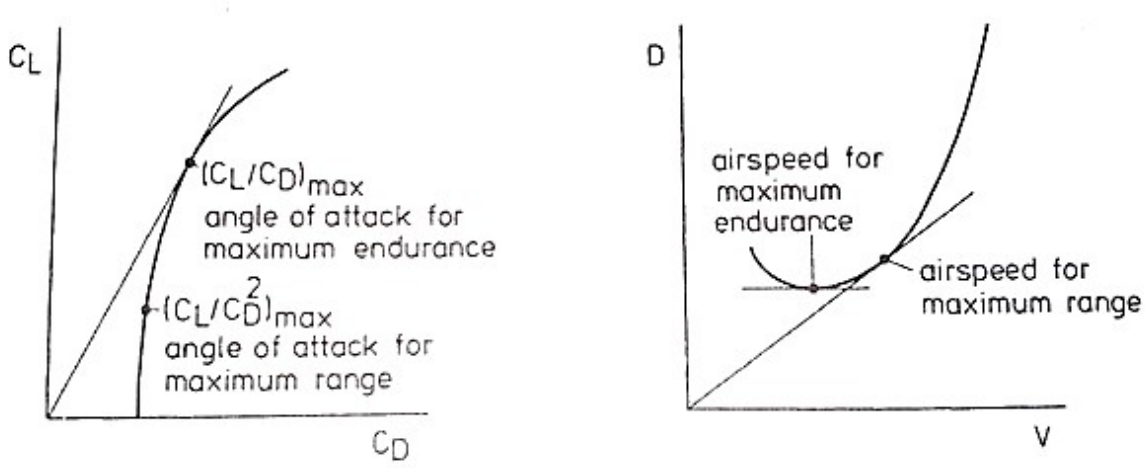

Figure 3.1: Range vs Endurance for jet engine aircraft [21]

3.2.1. Expected Research Results

The results of the research will be formulated as a maximum achievable amount of fuel saved by implementing CDO and CCO at AMS. Correspondingly the capacity will be determined for the scenarios with these fuel savings. Eventually, a trade-off must be made between the fuel savings and the capacity at AMS, as earlier research has determined that fully implementing CDO at AMS will cause a decline in capacity of 50%[13]. This is an infeasible implementation of CDO at AMS and therefore it is likely a trade-off must be made. This trade-off will be done based on the results of scenario 4 whereby the capacity and fuel savings will be varied throughout this scenario. Eventually based on these results, a Pareto front will be established for this scenario to determine the trade-off between fuel savings and capacity.

Additionally, two variables are of significant impact on the simulation results namely: wind and aircraft weight. As it falls out of the scope of this research to vary these parameters for each scenario, the impact of these parameters will be analysed for one scenario specifically. This will be done in order to determine the impact of the parameters individually.

3.3. Methodology

As this research focuses on minimising the impact of aviation on the environment, the main goal is to reduce fuel consumption. To minimise fuel consumption, the aircraft must fly at a velocity and descent profile which minimises total fuel consumption. It might be intuitive to assume that this would occur at the maximum glide ratio as this would be the most efficient flight in terms of Drag. This is certainly the case for gliders which must maximise their energy potential at any given altitude and velocity by minimising their drag [22] [20]. However, for civil aviation it is not possible to shut down the engines during descent due to the inability to maneouvre sufficiently if required. As the engines can not be shut down, they will consume fuel when idle and also produce a small amount of thrust. The idle thrust amount is assumed to be around 7%, based on the International Civil Aviation Organisation recommendation for the average ground and taxi idle thrust levels.

However, as aircraft are continuously burning fuel, even when the engines are idle, it is imperative to take the time in the sky into account and therefore also accounting for the velocity increase generated by the increase in Thrust and thus fuel consumption. Or simply said, the Drag over Velocity must be maximised in this case as can be seen in Figure 3.1.

In order to get a better understanding of the fundamentals of this flight phase, the equations of motions for this flight phase are analysed. The corresponding assumptions are mentioned in the respective steps.It should be noted that this is not a formal derivation for the specific case of a civil aircraft decelerating gliding flight with partial thrust. The cases presented here are for parts of this flight manoeuvre which are then combined to give an overview of the impact of all the individual components of this specific manoeuvre. Firstly, the fundamental case of a pure glider is explained. After this the case where fuel consumption is taken into account in order to maximise range. Finally the decelerating aspect is taken into account. The resulting im-

pact of each of these individual components is shown in Figure 3.2.

The general equations of motion for symmetric flight are given by Equation 3.1 and Equation 3.2.

$$Tcos\alpha_T - D - Wsin\gamma = m\frac{dV}{dt} \tag{3.1}$$

$$L - Wcos\gamma + Tsin\alpha_T = mV\frac{d\gamma}{dt} \tag{3.2}$$

Where for gliders the Thrust T is zero. The acceleration is assumed to be zero both in horizontal and vertical direction. γ is the FPA which is negative for descending flights and will be replaced by its negative counterpart γ_d, D is the drag force exerted on the aircraft given by:

$$D = C_D\frac{1}{2}\rho V^2 S \tag{3.3}$$

$$C_D = C_{D_0} + \frac{Cl^2}{\pi Ae} \tag{3.4}$$

Where C_{D_0} is the zero lift drag coefficient and the second term is the lift induced drag. Thus, for steady descending flight for a glider:

$$C_D\frac{1}{2}\rho V^2 S = Wsin\gamma_d \tag{3.5}$$

$$L = C_L\frac{1}{2}\rho V^2 S = Wcos\gamma_d \tag{3.6}$$

Dividing the above equations results in:

$$tan\gamma_d = \frac{C_D}{C_L} \tag{3.7}$$

Using Equation 3.6 and Equation 3.7 the rate of descent (RD) can be found:

$$RD = Vsin\gamma_d = V\frac{C_D}{C_L}cos\gamma_d = \sqrt{\frac{W}{S}\frac{2}{\rho}\frac{C_D^2}{C_L^3}cos^3\gamma_d} \tag{3.8}$$

These quantities, V, γ_d, RD are mainly influenced by the angle of attack of the aircraft. As can be seen in Equation 3.8, in order to minimise the rate of descent, C_D^2/C_L^3 must be minimised, or C_L^3/C_D^2 must be maximised. This is of most importance if the pilot wants to maximise endurance. If the pilot wants to maximise range, the FPA must be minimised and thus, as can be seen from Equation 3.7, C_L/C_D must be maximised. Although weight is of no influence to this term in itself, it is of influence on the airspeed and lift coefficient.

In the instance that there is a $Thrust$ component, the derivation is not similar. First, the equations for range for steady horizontal flight are investigated for jet aircraft, for which it is assumed that $Thrust$ is equal to the $Drag$. Fuel consumption is then defined as:

$$f = \eta T = \eta D \tag{3.9}$$

Where η is the thrust-specific fuel consumption and f the fuel flow. To maximise range, the fuel flow per unit velocity must be minimised. Thus:

$$(\frac{F}{V})_{min} = \frac{\eta D}{V} \implies (\frac{D}{V})_{min} \tag{3.10}$$

Assuming steady horizontal flight, this can be rewritten to:

$$(\frac{D}{V})_{min} = (\frac{D}{L}L\frac{1}{V})_{min} = (\frac{C_D}{C_L}W\frac{1}{V})_{min} \tag{3.11}$$

$$(\frac{D}{V})_{min} = \frac{W}{\sqrt{\frac{W}{S}\frac{2}{\rho}(\frac{C_L}{C_D^2})_{max}}} \implies (\frac{C_L}{C_D^2})_{max} \tag{3.12}$$

However, for a CDA this is not applicable and the situation more complex. First of all, Thrust is neither negligible like the glider example, nor equal to the amount of Drag that the aircraft encounters like the cruise

example above. Second, the aircraft will also be decelerating along its descending path from ToD to the FAF. This deceleration has a significant effect on the FPA.

In order to further investigate the impact of these parameters on the gliding performance of an aircraft, a numerical example is provided of the A320, one of the most prevalent aircraft types at AMS to implement decelerating flight, without Thrust T, Equation 3.1 reduces to:

$$D = W sin\gamma_d - m\frac{dV}{dt} \implies W sin\gamma_d = C_D \frac{1}{2}\rho V^2 S + m\frac{dV}{dt} \tag{3.13}$$

For the vertical equations of motion, there are no changes compared to the glider case described in Equation 3.6. When small angle approximation is applied for FPA up to 3°, $cos\gamma_d = 1$ and thus, the equation can be solved for the corresponding velocity when iterated over a range of C_L. In order to solve Equation 3.13 for the FPA, the deceleration must be determined. In this instance, the deceleration is assumed to be constant for a flight from cruise speed to the final approach speed. This results in the corresponding FPA for this decelerating flight path at different velocities. When Thrust T is applied, the simplification is made that the Thrust is 10% of the Drag D. Finally, the combined case is made where both a decelerating descent with Thrust is plotted. The resulting FPA can be found in Figure 3.2.

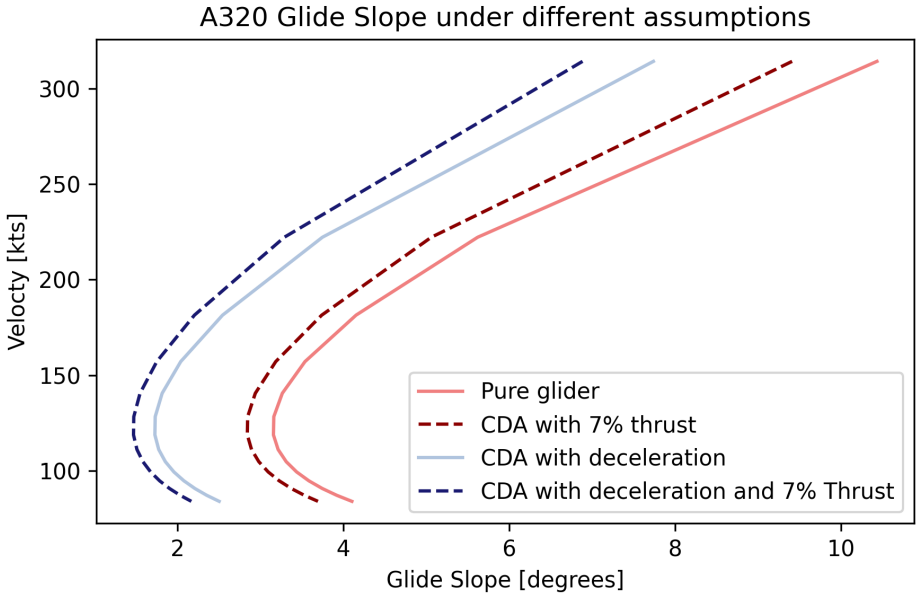

Figure 3.2: FPA comparison

Therefore, the FPA chosen in this research will be determined based on literature. As the focus of this research is on a practical implementation of CDO in a future scenario, further optimisation of the specific trajectories is considered out of scope. A difference will be made however between the different types of aircraft as this is of large impact on the FPA. There have been multiple studies on the matter of optimum FPA for fuel consumption such as Turgut, 2019 [29], who state that the highest fuel savings are noted at a FPA of 2.5°. Similarly, Inaad, 2016 [11] found a similar figure with the FPA varying between 2.0° and 2.6° for most aircraft. Research finds that fuel optimum FPA is most often more shallow then the current baseline implementation of ILS systems at Airports which mainly use a FPAof 3°. Comparing these numbers for the FPA corresponding the FPA for $(C_L/C_D)_{max}$ of most civil aviation aircraft, $(C_L/C_D)_{max}$ of most civil aviation aircraft lies between 15-18, which corresponds to a FPA of 3.8° and 3.2°.

4
Experimental Setup

This chapter will discuss the experimental setup that will be created in order to simulate the different scenarios described in section 3.2. Additionally, the parameters, data analysis and input to the simulation will be further explained. First, section 4.1 explains the setup of the simulation, followed by section 4.2 where the process of filtering and editing the Automatic Dependent Surveillance-Broadcast (ADS-B) data is explained. Finally, the used simulation parameters are given in section 4.3.

4.1. Simulation Set-up

The main set-up for this experiment consists of making use of the real-time Air Traffic Management Software Bluesky[1]. In order to simulate actual traffic, actual operations of aircraft must be extracted and processed in order to simulate this and to create a baseline of air-traffic at AMS on a busy day and the corresponding flight paths. Additionally, the simulation software can make use of multiple aircraft performance databases. In order to be fully transparent, the author will use OpenAP[2] [24]. This is an open source aircraft performance database which is able to accurately model most common aircraft at AMS. It was also considered to use Eurocontrol's Base of Aircraft Data (BADA), one of the most used aircraft performance models in the world. This is a total energy model and can be used for implementation in Bluesky. BADA is licensed under Eurocontrol and therefore not open source.

4.1.1. OpenAP usage

For this research, the OpenAP database will be used [24] which is compatible with Bluesky. It contains aircraft data based on open aircraft surveillance data and open literature models. The models consist out of four core components: aircraft and engine properties, dynamic performance, utilities such as navigation, and kinematic performances [26]. It should be noted that not all aircraft are part of this database and as such, in some instances a comparable aircraft must be chosen to simulate instead. For the research results this will be of limited impact as the research is about the relative difference between the base case scenario and the other scenarios. If an aircraft is replaced by an alternative, it is assumed that the relative change in fuel consumption will be similar.

4.1.2. Extension of Simulation Software

In order to successfully implement CDO procedures, the simulation software Bluesky needs to be extended where the aircraft are able to vary the FPA to the optimal aerodynamic FPA, compensating for current wind conditions. Additionally the desired acceleration during the descending flight must be added as a variable, currently Bluesky uses a default fixed acceleration or deceleration. The minimum thrust must also be changed as for a descending flight the default value in OpenAP is considered to be 15% of the thrust in flight. According to previous experiments done with Bluesky, the thrust parameter in Bluesky can be larger then it is in reality based on FMS data and must be decreased, as well as the corresponding fuel flow [9]. The autopilot module must be updated as well in the descent module where the current rate of descent is put to a default value of 3000 ft per 10 nm. This must be updated to reflect the actual corresponding rate of descent determined by the aerodynamic FPA, current wind conditions and aircraft weight

4.1.3. Simulation border

In order to evaluate the proper impact of the simulation, the simulation must start at a distance such that all aircraft are able to implement a full CDA from the start of the TMA and such that it can be evaluated what

[1] https://github.com/TUDelft-CNS-ATM/bluesky
[2] https://github.com/junzis/openap

the impact of CCO is. Due to speed restrictions, the main limiting factor is currently the levelling-off of these aircraft during climb at an altitude of 10,000ft. The border of the simulation has been determined by two factors, the minimum FPA for aircraft that land at AMS and the new upper border of the TMA of the Netherlands as proposed by Programma Luchtruimherziening. The minimum FPA from research was found to be around 2° [9] [11] [29]. The upper border of the TMA has been determined to be at 7,500m or around 25,000 ft. Therefore, using the minimum FPA and the upper border of the TMA results in a border with a radius of 215km centered around AMS. Do note, this does not mean that all aircraft start their descent immediately at the border, if an aircraft has a steeper geometric flight path than 2°, the aircraft will continue flight at its cruising altitude and starts the descent later such that the aircraft can follow its ideal descent path.

Due to the range of the ADS-B receiver, it was considered to place the border further away. However, this was deemed infeasible due to the large amount of extrapolation that would be required for the aircraft data. This will be explained in further detail in section 4.2. A figure of the borders that were considered can be seen in Figure 4.1, where the two additional borders that have been plotted, one for a FPA of 2° at an altitude of 35,000ft (the blue line) and one with the same FPA at an altitude of 21,000ft. The yellow dashed border indicates the chosen border for the simulation with a FPA of 2° at an altitude of 25,000ft.

4.1.4. Weight distribution

As the aircraft weight is an important factor in the glide velocity and thus the maximum range of the aircraft, it is important to take variations of the aircraft weight into account. The aircraft weight estimation is based on literature. Where the weight distribution is based on the OEW and Maximum Landing Weight (MLW) and is based on the work in Bouwels, 2021 [1]. The mass of the aircraft is also very important for the fuel consumption, as it has been reported that a 500kg difference in takeoff mass can account for an additional 40kg of fuel consumption for narrow-bodied aircraft [23]. The selection of aircraft types fall within 95% of all aircraft types at AMS and is further explained in subsection 4.2.1. The final table of the weight distribution per aircraft type and distribution can be found in Bouwels, 2021 Table A.1.

4.1.5. Wind implementation

Wind is a large factor and one of the main uncertainties for implementation of CDO [17] [30]. Therefore it is important that wind is incorporated in the simulations and that different wind conditions and corresponding changes in runway layout are analysed. Wind is a large factor due to the notion of an ideal FPA that is required for fuel optimal CDO. This is an aerodynamic angle, with respect to the aircraft and not with respect to the ground which is currently used for the ILS. This makes the approach procedure more complex.
For implementation of the wind conditions at each corresponding day, Global Forecast System (GFS) data is used. The wind conditions per scenario will be roughly similar and no large variations across different latitude and longitudinal positions will be used. The same holds for variations of wind speeds at different altitudes.

4.2. ADS-B Data processing

The ADS-B data used for this research is gathered from an ADS-B receiver on the roof of the faculty of Aerospace Engineering at the Delft University of Technology. The data from this receiver is freely accessible for anyone[3]. ADS-B data reports through semi-regular interval the following of an aircraft: Latitude, Longitude, ICAO identification number, Unique aircraft ID, Ground Speed, Track, Altitude, Rate of Climb and callsign.

Using ADS-B Data has the benefit of being freely accessible, unfortunately the quality of the data can sometimes vary significantly. Both in the accuracy of the data in terms of latitude, longitude and irregular time-steps. Similarly there are discrepancies with the values reported for Altitude and Ground Speed of which for some aircraft this is rarely received correctly. Therefore, the received data must be filtered and processed before it is useful for the simulation, this process is explained in subsection 4.2.2.

Additionally, the receiver has a limited range. Being located to the south of AMS, means aircraft coming from the North and more specifically using STAR EELDE - ARTIP and NARSO ARTIP as can be seen in Figure 2.5, are detected too late in order to stay outside of the simulation border. These aircraft must be extrapolated to the border of the simulation, this process is described in subsection 4.2.3. This effect is increased due to the lower altitude of aircraft at these points and the curvature of the earth, decreasing the range at which the signal of these aircraft is received even further. For one day during the summer of 2019, the points

[3] https://surfdrive.surf.nl/files/index.php/s/KYTR1ldO6vqCxXG

at which aircraft make first contact with the receiver are plotted in Figure 4.1. Where in general, the aircraft that are closer to AMS are flying at a lower altitude. This is for all aircraft that land at AMS that day, not taking departing aircraft into account.

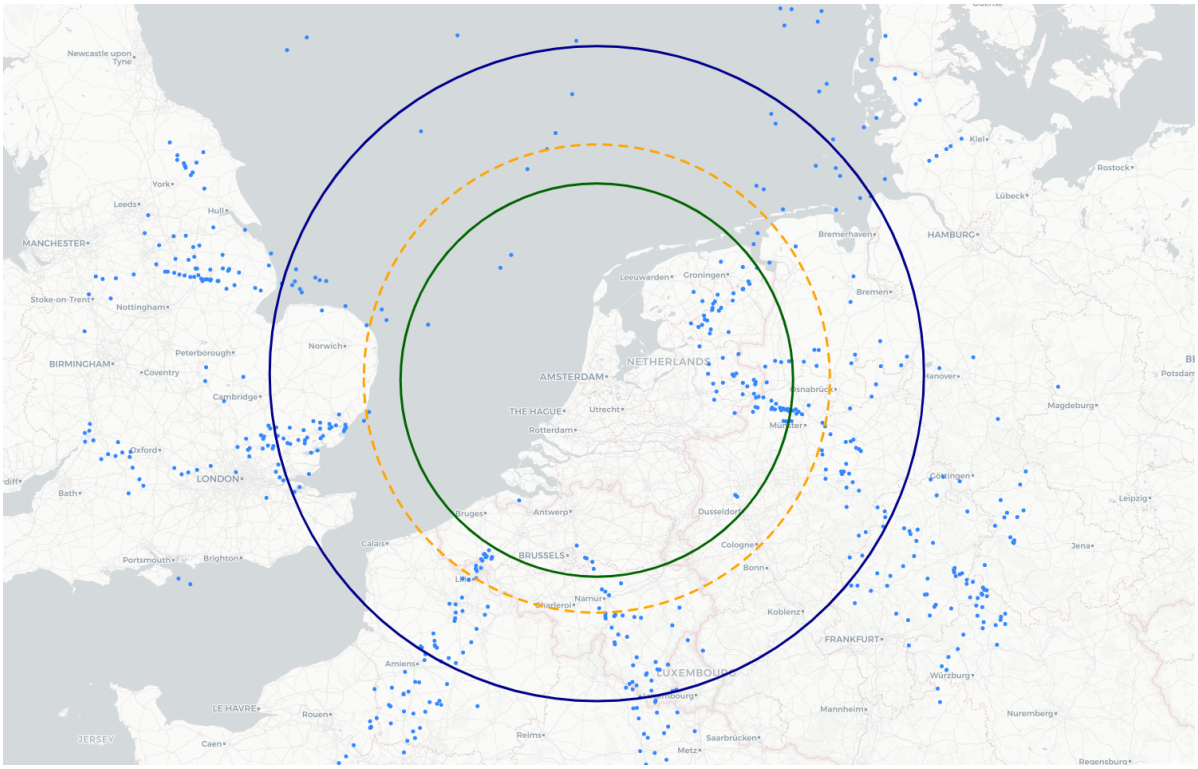

Figure 4.1: Example of ADS-B data: First point of contact of all aircraft landing at AMS in one day

4.2.1. Identifying aircraft types

The ADS-B data reports two types of identities, the ICAO identification number which is directly linked to the acADS-B receiver on the aircraft, and the unique aircraft identifier given by the receiver. This is beneficial when working with the data as some aircraft will have multiple return flights to AMS, this can be avoided by sorting on the unique aircraft identifier [25]. The aircraft unique identifier must be linked to ICAO identification number from which the aircraft type can be retrieved. As for the simulation it is required for the correct aircraft to be simulated. In order to map the ICAO identification numbers to the correct aircraft type, two databases are used. One is the Open Sky database[4] and contains over 460 thousand aircraft frames. The other is the Junzi Sun World Aircraft Database [5] and contains over 160 thousand frames. Unfortunately the latter has stopped updating in 2018 but the data recorded is still useful for the frames flying around right now. Using the data of multiple days, with around 630 unique aircraft per day, the Opensky Database can identify around 93% of all aircraft. The Junzi Sun World Aircraft Database can identify around 87% of all aircraft. When both databases are combined, the resulting is able to identify almost 96% of all aircraft. The remaining aircraft that cannot be identified by the ICAO identification number, will be assigned a random aircraft from the top six most common aircraft types at AMS currently [9], consisting of: B738, E190, A320, B737, A319, E75L. Together these aircraft cover over 60% of all incoming flights at AMS.
During simulation runs, it is also possible that the identified aircraft are not in the database from OpenAP, as this is a limited database, and as such are replaced by the closest similar aircraft type. For a typical simulation run, B77L is replaced by a B77W and B763 is replaced as well by a B77W. No other changes have been noticed so far in the assigning of the aircraft type.

[4] https://opensky-network.org/datasets/metadata/
[5] https://junzis.com/adb/

4.2.2. Filtering data

Only relevant data is required for the simulation, meaning aircraft departing from and landing at AMS. Aircraft are sorted on their unique aircraft id and by time, additionally aircraft are filtered according to the following criteria:

- Only aircraft that have more then 300 data points recorded
- Only aircraft whose first point of contact with the ADS-B receiver is more then 100km away.
- Only aircraft whose last point of contact is below 3000ft and first point of contact is above 5000 ft.
- Lastly, to make sure the aircraft is landing at or departing from AMS. Aircraft are filtered on their final or first data point and its proximity to AMS.

Filtering the data based on the requirement that the aircraft is at least 100km away is required as the simulation border is around 215km from AMS. If aircraft are less then 100km away, often indicating extremely short flights, small aircraft, or insufficient data, the aircraft will not be used for the simulation. Extrapolation to the border of the simulation of these aircraft is considered too volatile. The number of aircraft (also helicopters) that fall in this category is limited, around 25 aircraft on a busy day amounting to around 5% of all incoming flights. The impact on the maximum capacity for the simulation is therefore limited. It can also be noted that with the planned opening of Lelystad Airport[6] these type of aircraft will shift more towards Lelystad due to the limited capacity at AMS.

4.2.3. The extrapolation process

In order to simulate the benefits of implementing CDA procedures within the border of the TMA, some aircraft must be extrapolated to the edge of one of the border. The circles displayed in Figure 4.1, represent the distance from AMS if aircraft were to start their CDA at an FPA of 2.0°, the lowest possible FPA observed in literature, at differing altitudes. The lowest possible FPA has been chosen in order to give room for all aircraft to fully optimise their CDA to AMS, the FPA is relative to the aircraft and thus differing wind conditions can have impact on this. The blue line indicates an altitude of 35,000 ft, the typical cruise altitude, the orange dotted line is at an altitude of 25,000ft or 7.5km as indicated as the upper boundary of the TMA per the new proposal for luchtruimherziening NL [7]. The green line indicates the start of a CDA at an altitude of 21,000 ft. Hence, the further away the start of the CDA, the larger distance aircraft within this border will have to be extrapolated, which create additional uncertainty.

As can be seen in Figure 4.1, all aircraft that are within the large circle are within the border of the simulation. In order to solve for this, these aircraft will be extrapolated back towards the edge of the border. This will be done by comparing the aircraft to similar aircraft types and their relative path.

In order to extrapolate the position of the aircraft, the relative bearing θ is used between the first known point and five points later. This is done in order to determine the relative bearing on route to AMS. It has also been tested with the bearing between the first known point and AMS, but the results were deviating too much with respect to the path and heading of current aircraft routes. The difference between these two bearings can be seen in Figure 4.2 and Figure 4.3. The bearing is determined through Equation 4.1.

$$\theta = atan2(lon_5 - lon_1, lat_5 - lat_1) \tag{4.1}$$

Then, the corresponding new position is iterated with steps of size n in km, in this instance 1 km, to determine the new latitude and longitude position for each iteration step. Simultaneously, every 5 iteration steps, the coordinates are placed in the data set for the simulation of the aircraft in order to have the same interval of data points as the simulation. To determine the new latitude and longitude, the following equations are used where R_e is the mean radius of the earth, 6371km:

$$newlat = asin(sin(lat_1/180 * \pi) * cos(\frac{n}{R_e}) + cos(lat_1) * sin(\frac{n}{R_e}) * cos(\theta)) \tag{4.2}$$

$$newlon = lon_1 + atan2(sin(\theta) * sin(\frac{n}{R_e}) * cos(lat_1), cos(\frac{n}{R_e}) - sin(lat_1) * sin(newlat)) \tag{4.3}$$

As can be seen from Figure 4.4, not only aircraft whose first way-point is within the border needs to be placed on the border. As some aircraft have a sparse set of data at the border, these aircraft need some interpolation to be placed exactly on the border, similarly to the other aircraft. Otherwise there would still be a difference in distance from AMS per aircraft depending on the quality of the ADS-B data received. When this is done, all aircraft from Figure 4.1 are placed on the border wall as can be seen in Figure 4.5.

[6] https://www.rijksoverheid.nl/onderwerpen/luchtvaart/ontwikkeling-lelystad-airport

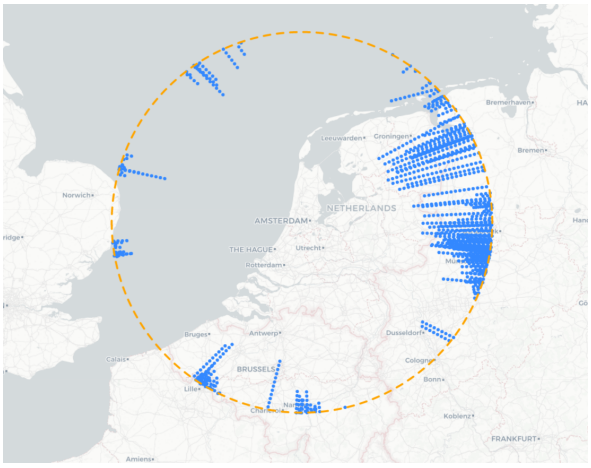

Figure 4.2: Extrapolation of aircraft to the simulation border using bearing with respect to AMS

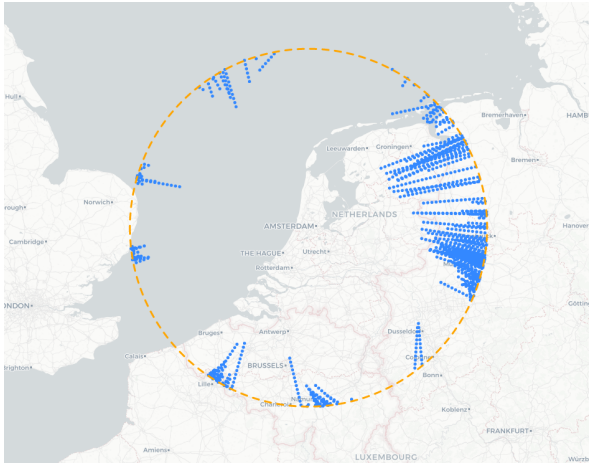

Figure 4.3: Extrapolation of aircraft to the simulation border using bearing with respect to its own route

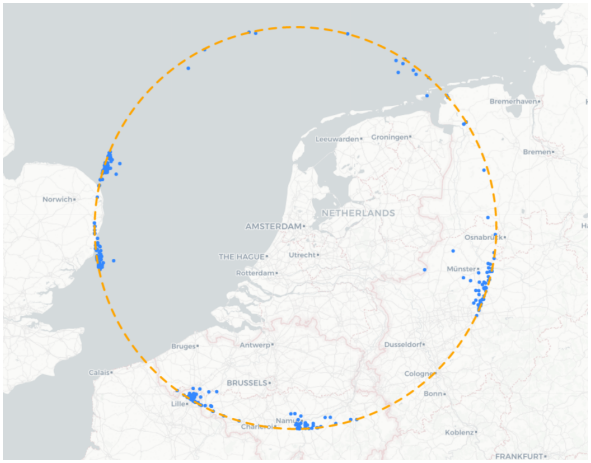

Figure 4.4: All aircraft initially outside of border, first way-point placed inside the border

Figure 4.5: All aircraft placed on border as starting point for the simulation

After the position of the aircraft on the border has been determined with the corresponding way-points by extrapolation, the velocity and altitude needs to be determined at those way-points. In order to do this, the border of the simulation is divided into several radials, each corresponding roughly to the current STARs in place for AMS. The exact radials that have been determined are to some extent chosen arbitrarily and can easily be adapted to fit other values if the reader deems that more suitable. The division of the currently used radials can be seen inFigure 4.6. The radials have been created in order to more accurately simulate a scenario for which the aircraft operate based on the entry points of the aircraft on their bearing. Meaning, aircraft coming from the East might have a different altitude and velocity due to commands from ATC in Germany compared to aircraft coming from the West whom have been given altitude and speed commands from other controlled airspace. Each section collects the data from aircraft on the border. Only aircraft that had data points outside of the border were used for this. For each sector, the altitude and ground speed for the aircraft was averaged, this had been done for all aircraft in one day. After this, the aircraft that are extrapolated to the border use a linear scale from their current ground speed and altitude to the average ground speed and altitude at the border.

4.3. Simulation Parameters

Simulations will take place on multiple different days to account for different wind conditions and runway layouts. The days to be simulated will be picked from busy days during the summer of 2019 to be as close to peak capacity as possible. As the requirement to carry an ADS-B receiver was only mandatory from January

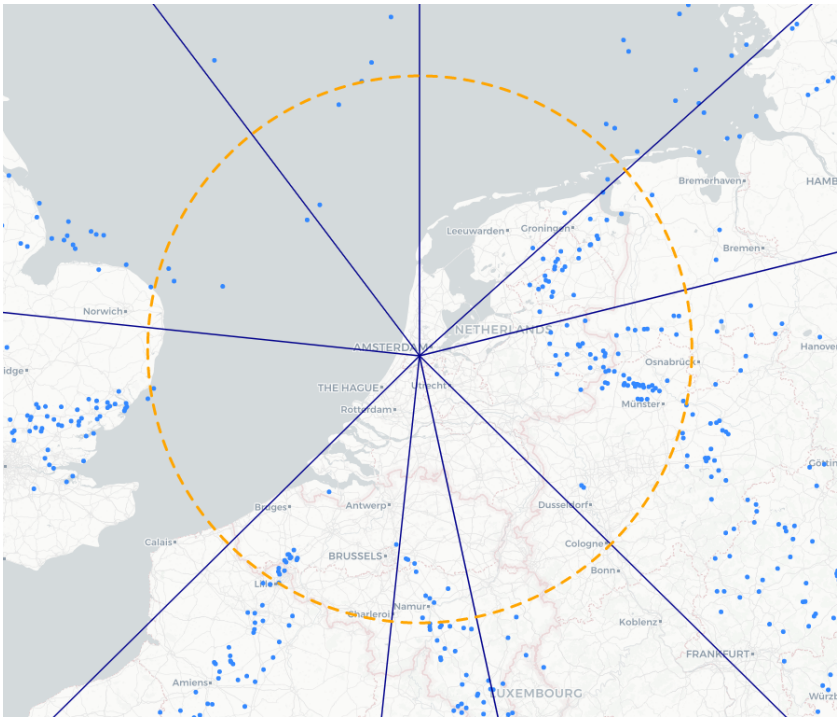

Figure 4.6: Radials determined for extrapolation of aircraft altitude and velocity

1st, 2020 onward and the decrease in air traffic that follows from that period, it is determined to use a peak period as close to January 1st, 2020 in the presumption that most aircraft would have an ADS-B receiver on board.

Therefore, the parameters that will be varied are: wind speed, aircraft weight, runway layout and the different scenarios defined. The scenarios that will be tested are described in section 3.2.

Additionally, wind will be varied for one specific scenario to determine the impact of a southern wind of 10kts or 20kts in terms of capacity and fuel consumption. Wind is also taken into account in regard to runway layout and the day the simulation takes place. But it will not be part of further analysis for each specific scenario. Aircraft weight will be varied as well, this will be done according to the method described in subsection 4.1.4. Similarly to the variation wind, the impact of differing weight will be analysed for one specific case to determine the impact of this variation. It will not be a core part of each analysis on the scenarios.

4.3.1. Scenario runs

All scenarios where separation is taken into account, will be simulated in real time in order to be able to vector the aircraft. This will be done using point merge and late merge techniques first and foremost, after which speed commands are considered if no alternatives are viable along the aircraft path. Ideally this process would be automated, however for this research such an application was considered to be out of scope. In order to ensure separation, an Airborne Separation Assurance System tool already implemented in Bluesky will be used in order to monitor the aircraft. If a conflict is detected, aircraft will be vectored.

4.3.2. Simulation flowchart

In Figure 4.7, a flowchart is presented which shows the process of the simulations. First, based on wind data, weight distribution of aircraft and on ADS-B data from some relevant days in the past, a time-based prediction will be made per aircraft to determine the order of their arrival and possible conflicts during the descent. After this, if aircraft have a lateral path optimisation, aircraft will take the shortest path to AMS, if not the aircraft will follow the lateral path as defined by the ADS-B data. All of these will generate the corresponding scenario file. This scenario file will be run in Bluesky for which it must be determined if separation is of influence for this run or if it is only necessary to determine the theoretical optimal fuel savings. If separation is required, the simulation will be run real-time in order to vector the aircraft and maintain separation where the researcher

will act as the ATC. The resulting simulation run will generate the relevant output in terms of capacity and fuel. In Figure 4.7 an overview of this process is shown.

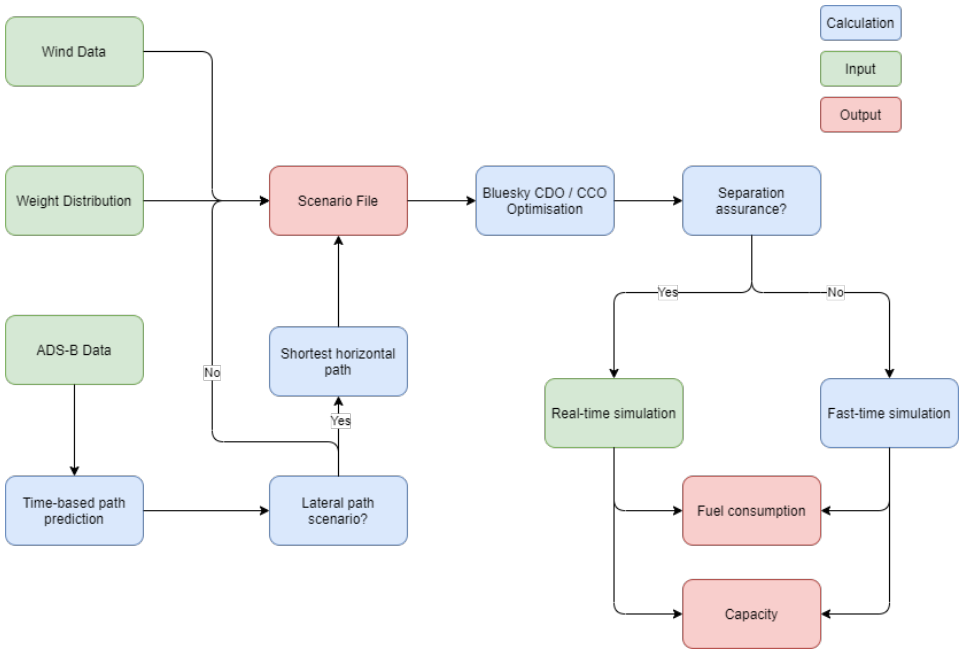

Figure 4.7: Code flowchart

5
Preliminary simulation results

In order to verify the correct implementation of the ADS-B data, the ADS-B data as input is compared to the Bluesky data as output. In section 5.1 the two are compared. In section 5.2, the extrapolation of the ADS-B data is analysed as well as the approach path from the ToD from the different radials from AMS. Finally, in section 5.3 the first results of the fuel consumption of aircraft is presented as well as the impact of wind on the total fuel consumption.

5.1. ADS-B Data comparison

To analyse the resulting ADS-B Data input to the corresponding Bluesky output, a plot was made per aircraft comparing the altitude and ground speed input to the output from Bluesky. As can be seen from the example in Figure 5.1 for an B737; the input matches the output very similarly. There are examples where this is not the case. For example in Figure 5.2 where the ADS-B data is inaccurate and as a result gives conflicting input to Bluesky. The resulting flight path in Bluesky is one that the aircraft is not able to follow and as such the aircraft does not make the final approach path to AMS. This means that the data needs to be filtered additionally for consistency errors.

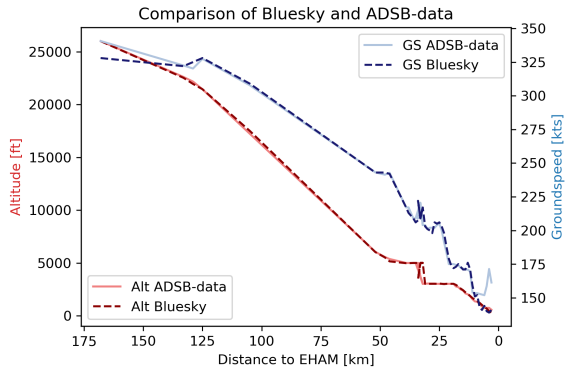

Figure 5.1: Example of accuracy in some instances of the simulation

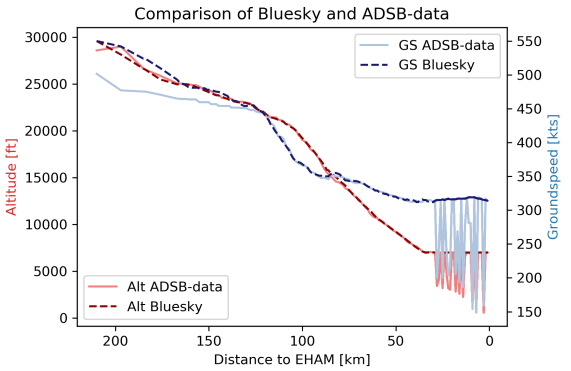

Figure 5.2: Example of sensitivity of ADS-B data

5.2. Comparison of ADS-B data extrapolation to Bluesky

In this section, the altitude between Bluesky and the ADS-B data per sector is compared as shown in Figure 4.6. As aircraft coming from the east are extrapolated more often, the results are verified in order to make sure aircraft are able to follow the commands given and the way-points that were extrapolated as explained in subsection 4.2.3. When looking at the figures in Appendix B and more specifically Figure 5.3 and Figure 5.4, two things stand out. Firstly, the aircraft for the radial between 60° and 80°, and similarly for the radial between 190° and 240°, show an over representation of a linear altitude decrease for the first section of the descent. This corresponds with the number of aircraft from these tracks that have been extrapolated back to the border. Secondly, it is noticed that there is some error in the data with some outliers exceeding an altitude of 45,000ft at the border of the simulation. This must be investigated further for additional filtering of the ADS-B data.

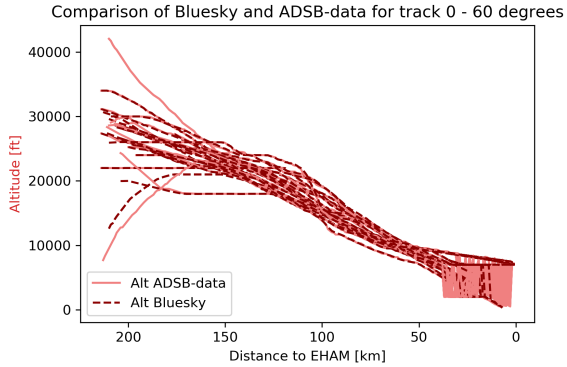

Figure 5.3: Comparison of ADS-B data and Bluesky sim for track 0 - 60 degrees, containing 21 aircraft

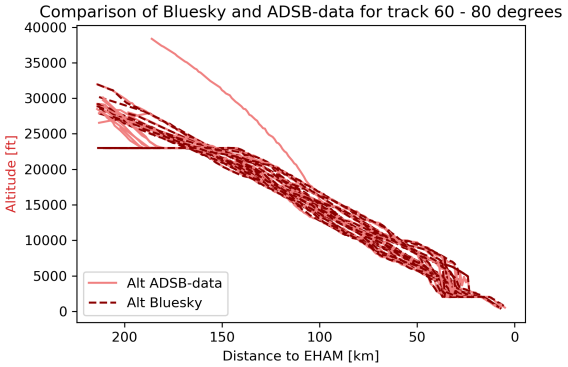

Figure 5.4: Comparison of ADS-B data and Bluesky sim for track 60 - 80 degrees, containing 19 aircraft

5.3. Fuel consumption preliminary figures

The fuel consumption of the flight in Figure 5.1 is shown in Figure 5.5 and Figure 5.6. In these figures, it can be observed that during the level-off phase at around 7,000 ft, the fuel consumption increases. This is a typical behaviour for aircraft at AMS as after the final way-point from the STAR, they are often levelled-off quickly at 7,000ft or 3,000ft for the final approach. This shows the impact of a longer section of level flight in terms of fuel consumption. It should be noted that the distance to AMS is the absolute distance from the point and not the along track distance. Thus for the final approach where aircraft turn towards the runway, this means there is a longer section of flight with the same distance from AMS. In Figure 5.6, the fuel consumption for the same flight is plotted but in this scenario also wind was taken into account. In this instance there was a 10 kts headwind for the approach to runway 18R. The total fuel consumption for the scenario with a 10kts headwind was 800kg of fuel compared to a total fuel consumption of 730kg of fuel for the scenario without wind.

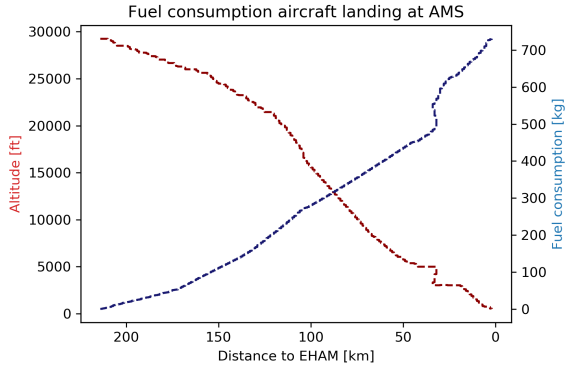

Figure 5.5: Cumulative fuel consumption for descending flight to AMS

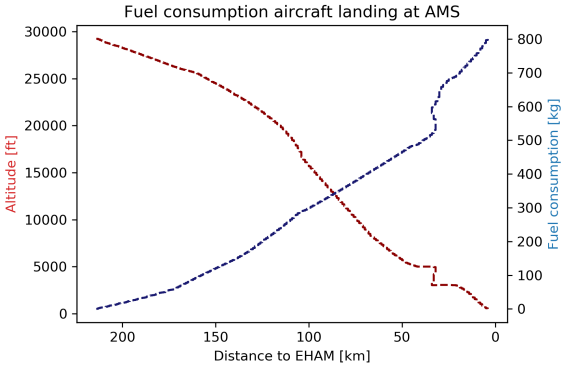

Figure 5.6: Cumulative fuel consumption for descending flight to AMS with a 10kts headwind

In Figure 5.7 and Figure 5.8 the instantaneous fuel consumption for the same two scenarios, with a 10kts headwind and without wind, is plotted along the distance from AMS. In this comparison it can be seen that due to the headwind, the levels of fuel and thus additional thrust, that was required for the aircraft to maintain its path increased during the initial phase of the descent. After this initial descent phase, it can not be determined from this figure whether the fuel consumption after this increased more heavily as well. Its mainly interesting to note how it influences the initial descent phase and thus highlighting the impact of wind on the initial descent phase.

For this simulation, in total 148 aircraft where simulated over a period of 3.5 hours where it starts at the beginning of the morning arrival peak and ends near the end of the departure peak. Two separate versions of this were run as mentioned above, one scenario with no wind conditions and one with a 10kts headwind.

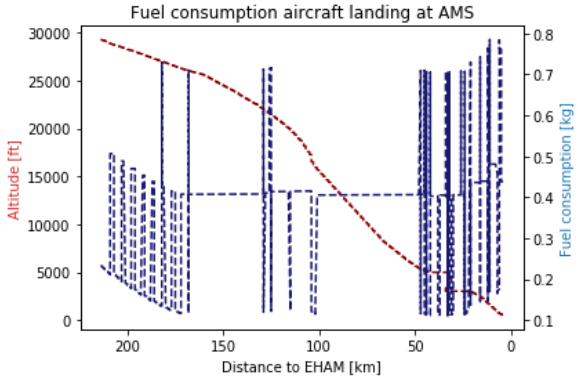

Figure 5.7: Cumulative fuel consumption for descending flight to AMS with a decrease in FPA

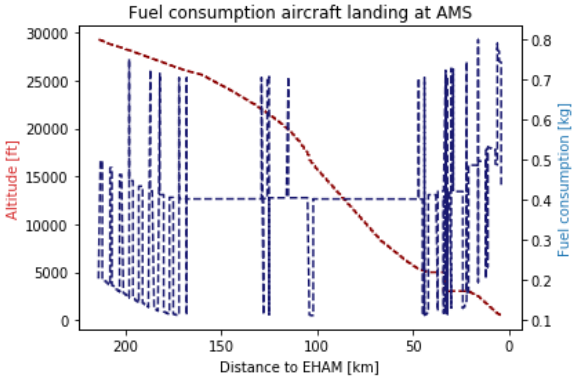

Figure 5.8: Instantaneous fuel consumption for descending flight to AMS with a decrease in FPA

The scenario with no wind had a total fuel consumption of 175 thousand kg. The scenario with a 10kts headwind had a total fuel consumption of 205.5 thousand kg, meaning an increase of over 17% of fuel due to the differing wind conditions. For the continuation of this research, more differing wind conditions will be tested as well as the specific added benefits of the different CDA implementations.

Bibliography

[1]

[2]

[3] Noise. URL https://www.heathrow.com/company/local-community/noise/operations/arrival-flight-paths.

[4] Heathrow implements world's first fully systemised optimised runway delivery tool with enhanced time based separation, Mar 2018. URL https://www.nats.aero/news/heathrow-implements-worlds-first-fully-systemised-optimised-runway-delivery-tool-enhanced-time-based-separ

[5] Eurocontrol five-year forecast 2020-2024. *https://www.eurocontrol.int/sites/default/files/2020-11/eurocontrol-five-year-forecast-europe-2020-2024.pdf*, Nov 2020. URL https://www.eurocontrol.int/sites/default/files/2020-11/eurocontrol-five-year-forecast-europe-2020-2024.pdf.

[6] Economic impacts of covid-19 on civil aviation, 2020. URL https://www.icao.int/sustainability/Pages/Economic-Impacts-of-COVID-19.aspx.

[7] Herziening luchtruim, 2020. URL https://www.luchtvaartindetoekomst.nl/herziening-luchtruim/default.aspx.

[8] S. Alam, M. H. Nguyen, H. A. Abbass, Chris Lokan, M. Ellejmi, and S. Kirby. Multi-aircraft dynamic continuous descent approach methodology for low-noise and emission guidance. *Journal of Aircraft*, 48, 2011. ISSN 15333868. doi: 10.2514/1.C031241.

[9] B. Bouwels, J.M. Hoekstra, and J. Ellerbroek. Off-idle continuous descent operations at schiphol airport, Apr 2021. URL http://resolver.tudelft.nl/uuid:fa55d141-ea6d-4bb9-b463-515742e55935.

[10] J.M. de Wilde. Implementing point merge system based arrival management at amsterdam airport schiphol, 2018.

[11] J. Ellerbroek, Mazin Inaad, and J.M. Hoekstra. Fuel and emission benefits for continuous descent approaches at schiphol, Nov 2016. URL http://resolver.tudelft.nl/uuid:85153290-ac20-4005-8901-60d3861a8c75.

[12] J. Ellerbroek, Jeffrey Klapwijk, and J.M. Hoekstra. Potential fuel benefits of optimized continuous climb operations at schiphol, Feb 2018. URL http://resolver.tudelft.nl/uuid:bb6a8f8c-4cbd-4bba-adfb-0505eb049c54.

[13] Louis Erkelens. Research into new noise abatement procedures for the 21st century. 2000. doi: 10.2514/6.2000-4474.

[14] A. Errico and Vittorio Di Vito. Study of point merge technique for efficient continuous descent operations in tma. *IFAC-PapersOnLine*, 51, 2018. ISSN 24058963. doi: 10.1016/j.ifacol.2018.07.032.

[15] Eurocontrol. European cdo / cco action plan. Nov 2020.

[16] Michael Felux, Thomas Dautermann, and Hayung Becker. Gbas landing system - precision approach guidance after ils. *Aircraft Engineering and Aerospace Technology*, 85, 2013. ISSN 00022667. doi: 10.1108/AEAT-07-2012-0115.

[17] W. F. De Gaay Fortman, M. M. Van Paassen, M. Mulder, A. C. In't Veld, and J. P. Clarke. Implementing time-based spacing for decelerating approaches. *Journal of Aircraft*, 44:106–118, 2007. ISSN 15333868. doi: 10.2514/1.22253.

[18] ICAO. Continuous descent operations (cdo) manual, 2010.

[19] Ramon Gomez Ledesma, Francisco A. Navarro, and Bastian Figlar. Continuous descent approaches for maximum predictability. 2007. doi: 10.1109/DASC.2007.4391871.

[20] G.J.J Ruijgrok. *Elements of airplane performance.* Delft University Press, 2004.

[21] G.J.J Ruijgrok. page 290. Delft University Press, 2004.

[22] Donglong Sheu, Yu Min Ghent, Yuan Jen Chang, and Jeng Shing Chern. Optimal glide for maximum range. 1998. doi: 10.2514/6.1998-4462.

[23] Ernesto Staffetti, Alberto Olivares, and Manuel Soler. Multiphase optimal control framework for commercial aircraft four-dimensional flight-planning problems. 2015.

[24] Junzi Sun. junzis/openap. URL https://github.com/junzis/openap.

[25] Junzi Sun. *The 1090 Megahertz Riddle: A Guide to Decoding Mode S and ADS-B Signals*. TU Delft OPEN Publishing, 2 edition, 2021. ISBN 978-94-6366-402-8. doi: 10.34641/mg.11.

[26] Junzi Sun, Jacco M. Hoekstra, and Joost Ellerbroek. Openap: An open-source aircraft performance model for air transportation studies and simulations. *Aerospace*, 7(8), 2020. ISSN 2226-4310. doi: 10.3390/aerospace7080104. URL https://www.mdpi.com/2226-4310/7/8/104.

[27] Emmanuel Sunil. Analyzing and modeling capacity for decentralized air traffic control. *TU Delft University*, 2019.

[28] Raúl Sáez, Xavier Prats, Tatiana Polishchuk, Valentin Polishchuk, and Christiane Schmidt. Automation for separation with continuous descent operations: Dynamic aircraft arrival routes. *Journal of Air Transportation*, 28, 2020. ISSN 23809450. doi: 10.2514/1.D0176.

[29] Enis T. Turgut, Oznur Usanmaz, Mustafa Cavcar, Tuncay Dogeroglu, and Kadir Armutlu. Effects of descent flight-path angle on fuel consumption of commercial aircraft. *Journal of Aircraft*, 56, 2019. ISSN 15333868. doi: 10.2514/1.C033911. Alle info over GS voor verschillende vliegtuigen en bijbehorende brandstof besparingen door langere cruise flight

.

[30] Alexander C. In't Veld, René Van Paassen, Max Mulder, and John Paul Clarke. Pilot support for separation assurance during decelerating approaches. volume 3, 2004. doi: 10.2514/6.2004-5102.

A

Weight Distribution Aircraft

Table A.1: Weight Distribution across the 95% most common aircraft types from [1].

Aircraft Type	Estimated Mean Weight [Tonnes]	Estimated Weight STD [Tonnes]	P(LW <OEW)	P(LW >MLW)
B738	57.4	2.8	4e-09	0.001
E190	37.8	1.9	4e-09	0.000
A320	57.9	2.7	4e-09	0.008
B737	51.8	2.5	4e-09	0.005
A319	55.0	2.6	4e-09	0.004
E75L	30.2	1.4	4e-09	0.004
A333	167.0	7.8	4e-09	0.013
A321	66.3	3.2	4e-09	0.003
E170	28.3	1.4	4e-09	0.000
B744	246.1	12.0	4e-09	0.001
B77W	229.1	10.6	4e-09	0.018
B772	185.4	8.6	4e-09	0.016
B739	59.1	2.8	4e-09	0.004
B789	175.8	8.1	4e-09	0.019
B763	118.5	5.7	4e-09	0.001
A332	164.6	7.7	4e-09	0.014
B77L	199.5	9.4	4e-09	0.006
DH8D	23.4	1.2	4e-09	0.000
F100	33.4	1.6	4e-09	0.016
B788	162.0	7.3	4e-09	0.077
CRJ9	29.8	1.4	4e-09	0.006
A20N	58.5	2.8	4e-09	0.002
B748	284.7	13.2	4e-09	0.019
B733	45.3	2.2	4e-09	0.001
E195	38.3	1.9	4e-09	0.000

B

Preliminary results Aircraft Extrapolation

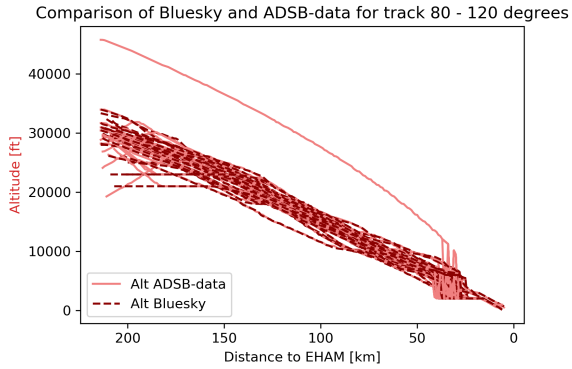

Figure B.1: Comparison of ADS-B data and Bluesky sim for track 80 - 120 degrees, containing aircraft

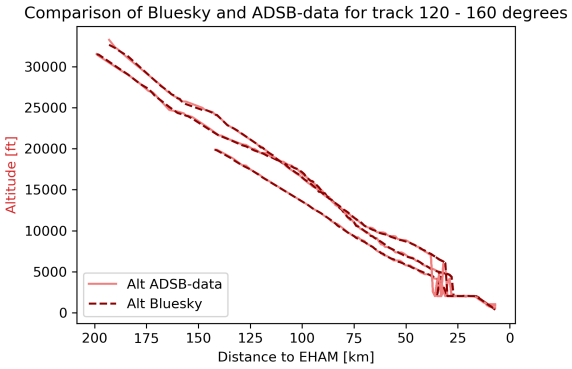

Figure B.2: Comparison of ADS-B data and Bluesky sim for track 120 - 160 degrees, containing aircraft

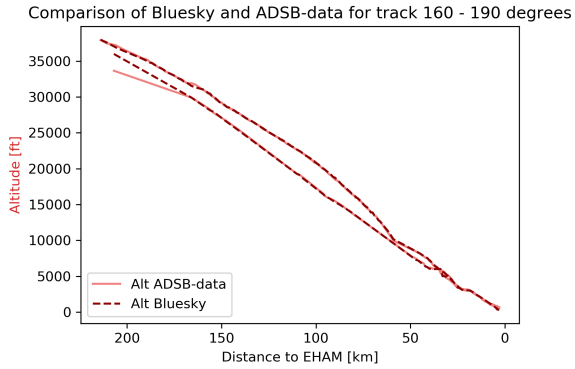

Figure B.3: Comparison of ADS-B data and Bluesky sim for track 160 - 190 degrees, containing aircraft

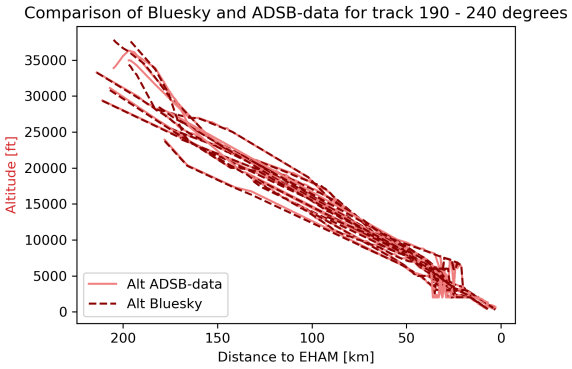

Figure B.4: Comparison of ADS-B data and Bluesky sim for track 190 - 240 degrees, containing aircraft

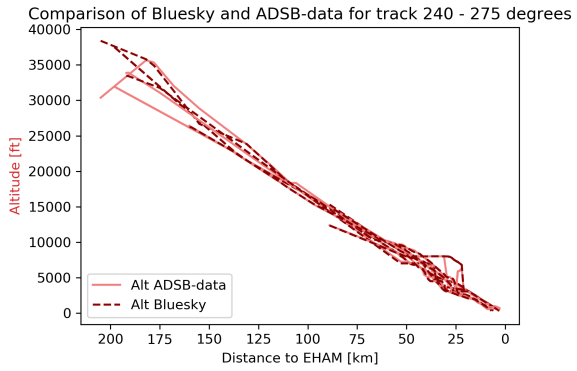

Figure B.5: Comparison of ADS-B data and Bluesky sim for track 240 - 270 degrees, containing aircraft

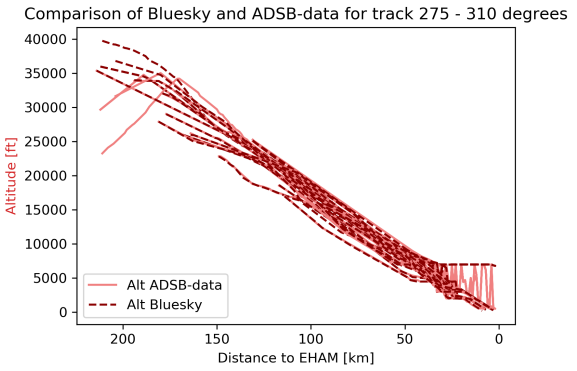

Figure B.6: Comparison of ADS-B data and Bluesky sim for track 275 - 310 degrees, containing aircraft

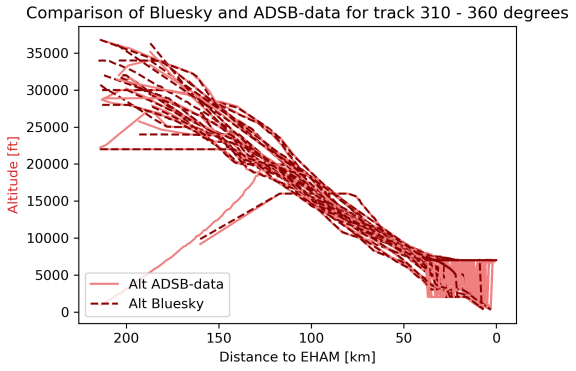

Figure B.7: Comparison of ADS-B data and Bluesky sim for track 310 - 360 degrees, containing aircraft